

The role of new Stokes curves in some physics problems

Akira Shudo

Department of Physics, Tokyo Metropolitan University

Outline

New Stokes curves appear in addition to the conventional Stokes curves in the Stokes geometry for high-order differential equations. New Stokes curves must also be considered when performing saddle point evaluation of integrals involving more than two saddle points. It would be fascinating to identify situations where these new objects play a significant role and predict new phenomena in physics. Here we explore this possibility through the following two examples:

1. Feynman propagator for the discrete dynamical systems
2. Multi-state non-adiabatic transition

Stokes geometry and new Stokes curves

3rd order differential equations

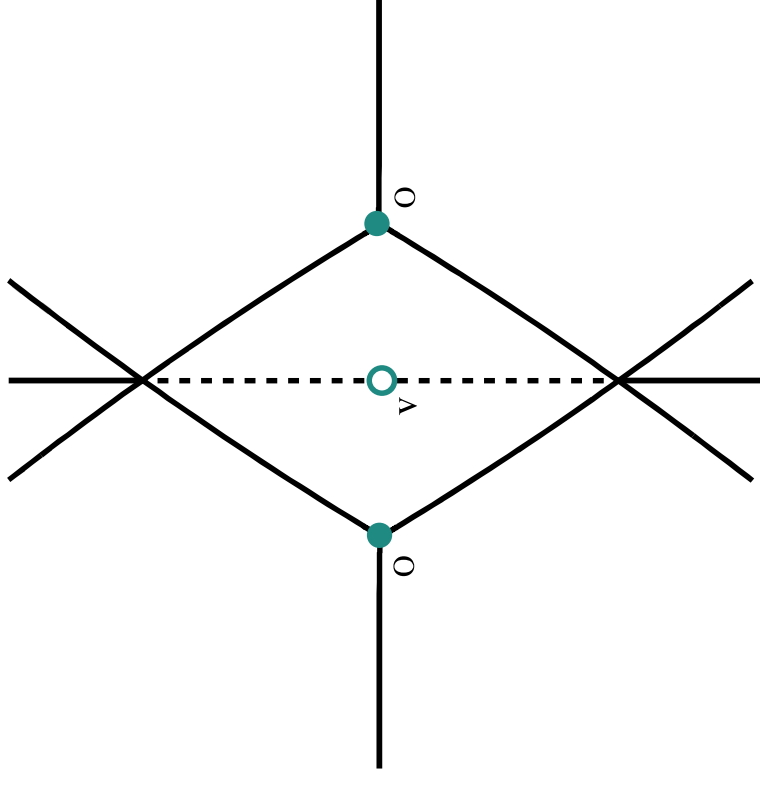
$$\left(\eta^{-3} \frac{d^3}{dz^3} + 3\eta^{-1} \frac{d}{dz} + \mathbf{i}z \right) \varphi = 0 \quad (\eta: \text{large parameter})$$

- Necessity to introduce *new Stokes curves*

(Berk, Nevins and Roberts, 1982)

- Introducing *virtual turning points* based on the exact WKB analysis

(Aoki, Kawai and Takei, 1994)



Stokes geometry and new Stokes curves

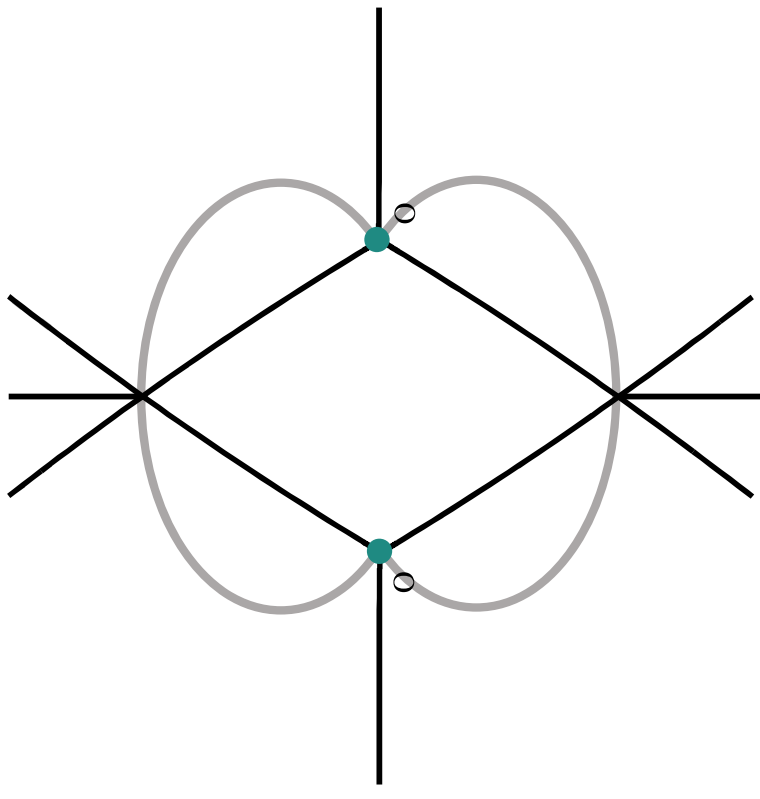
Integral with more than two saddles

$$f(x, y) = \int_{-\infty}^{\infty} \exp \left(i \left(t^4 + xt^2 + yt \right) \right) dt$$

- **Necessity to introduce *new Stokes curves***
(Berk, Nevins and Roberts, 1982)

- **Introducing *virtual turning points* based on the exact WKB analysis**
(Aoki, Kawai and Takei, 1994)

- **Introducing *higher-order Stokes phenomena***
(Howls, Langman and Olde Daalhuis, 2004)



Stokes geometry and new Stokes curves

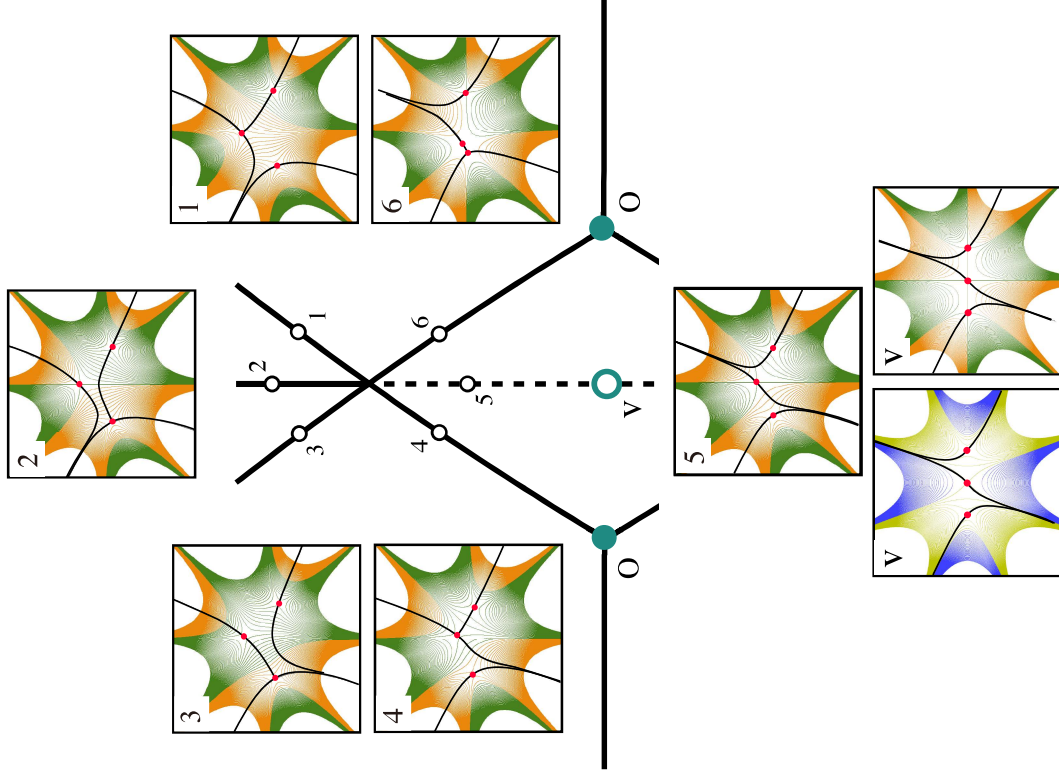
Integral with more than two saddles

$$f(x, y) = \int_{-\infty}^{\infty} \exp \left(i \left(t^4 + xt^2 + yt \right) \right) dt$$

- Necessity to introduce *new Stokes curves*
(Berk, Nevins and Roberts, 1982)

- Introducing *virtual turning points* based on
the exact WKB analysis
(Aoki, Kawai and Takei, 1994)

- Introducing *higher-order Stokes phenomena*
(Howls, Langman and Olde Daalhuis, 2004)



Feynman propagator for the discrete dynamical systems

Multiple integral in the form

$$u(q_0, q_n) = \int \cdots \int dq_1 dq_2 \cdots dq_{n-1} \exp \left(\frac{i}{\hbar} S(q_0, q_1, \dots, q_n) \right)$$

where

$$S(q_0, q_1, \dots, q_n) = \sum_{j=1}^n \frac{1}{2} (q_j - q_{j-1})^2 - \sum_{j=1}^{n-1} V(q_j)$$

Saddle point condition

$$\frac{\partial}{\partial q_i} S(q_0, q_1, \dots, q_n) = 0 \quad (1 \leq i \leq n-1)$$

gives the **area-preserving map** in the Lagrangian form

$$F : (q_{i+1} - q_i) - (q_i - q_{i-1}) = -V'(q_i) \quad \Leftrightarrow \quad F : \begin{pmatrix} p_{i+1} \\ q_{i+1} \end{pmatrix} = \begin{pmatrix} p_i - V'(q_i) \\ q_i + p_i - V'(q_i) \end{pmatrix}$$

Find the saddles on the real q_n -axis (q_0 fixed)

Hénon map

In the following, we take

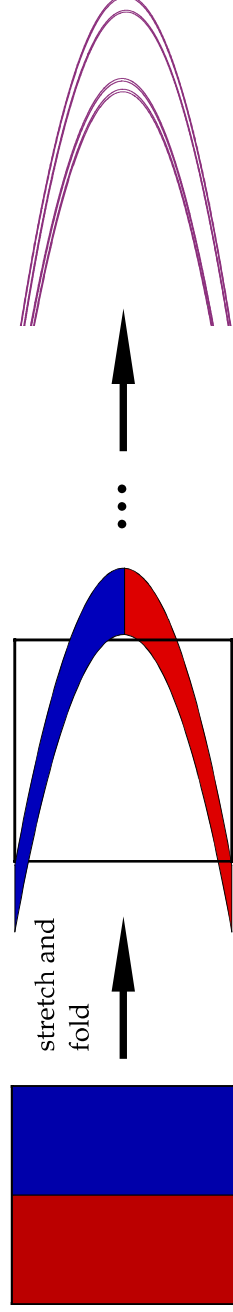
$$V(q) = -\frac{1}{3}q^3 - cq$$

where $c \in \mathbb{R}$ is a parameter. F is transformed via the affine change of the variables $(p, q) = (y - x, 1 - x)$ into one of the standard forms of the **Hénon map**

$$\mathcal{H} : \begin{pmatrix} x_{i+1} \\ y_{i+1} \end{pmatrix} = \begin{pmatrix} -x_i^2 - y_i + a \\ x_i \end{pmatrix} \quad (a = -c - 1)$$

Classification of 2-D polynomial maps (Friedland-Milnor)

Polynomial diffeomorphisms in 2-D are conjugate either to the elementary, affine or generalized Hénon maps. The former two are simple and well understood. Only the generalized Hénon map is non trivial as the dynamical system.



Anti-integrable limit

Introducing a new variable $q'_i = \epsilon q_i$ and a new parameter $\epsilon = 1/\sqrt{-c}$, the new action can be introduced as $\hat{S} = \epsilon^3 S$ where

$$\hat{S} = \epsilon \left\{ \sum_{j=0}^{n-1} \frac{1}{2} (q'_{j+1} - q'_j)^2 \right\} - \sum_{j=1}^{n-1} \left(-\frac{q_j'^3}{3} - q'_j \right).$$

As long as $\epsilon \neq 0$ the variational condition $\delta \hat{S} = 0$ is equivalent to the explicit mapping rule

$$F : (q_{i+1} - q_i) - (q_i - q_{i-1}) = -V'(q_i)$$

but in case $\epsilon = 0$, such **explicit relations no longer exist** between successive points. Nevertheless, the new action \hat{S} depends on ϵ analytically and the “orbits” for $\epsilon = 0$ are simply expressed as $q_i \in \{-1, +1\}$ ($i \in \mathbb{Z}$). Such a singular limit is called **anti-integrable limit**.

For $\epsilon = 0$,

$n = 1$: Airy

$n = 2$: direct product of Airy

...

Virtual turning points and new Stokes curves

— Differential equations case —

Higher-order differential equations with a large parameter η

$$P\psi(x,\eta)=\left(\frac{d^m}{dx^m}+q_1(x)\eta\frac{d^{n-1}}{dx^{m-1}}+\cdots+q_m(x)\eta^m\right)\psi(x,\eta)=0$$

Borel transform

$$P_B\psi_B(x,y)=\left(\frac{\partial^m}{\partial x^m}+q_1(x)\frac{\partial}{\partial y}\frac{\partial^{n-1}}{\partial x^{m-1}}+\cdots+q_m(x)\frac{\partial^m}{\partial y^m}\right)\psi_B(x,y)=0$$

Symbol

$$\sigma(x,\xi,\eta)=\xi^m+q_1(x)\eta\xi^{m-1}+\cdots+q_m(x)\eta^m$$

Hamiltonian-Jacobi equation:

$$\begin{aligned}\frac{dx}{dt} &= \frac{\partial \sigma}{\partial \xi}, & \frac{d\xi}{dt} &= -\frac{\partial \sigma}{\partial x} \\ \frac{dy}{dt} &= \frac{\partial \sigma}{\partial \eta}, & \frac{d\eta}{dt} &= -\frac{\partial \sigma}{\partial y}\end{aligned}$$

Virtual turning points and new Stokes curves

— Differential equations case —

Definition (Aoki-Kawai-Takei)

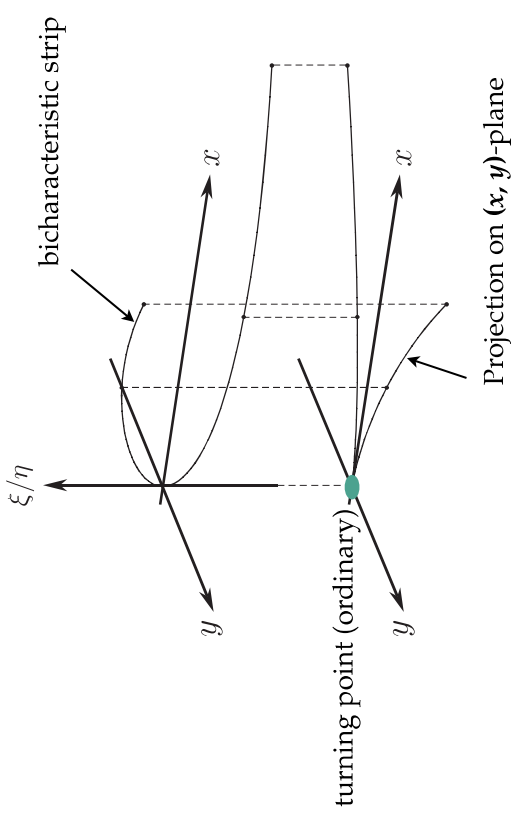
(i) A point $x = a$ is said to be an **ordinary turning point** if

$$\zeta^m + q_1(x)\zeta^{m-1} + \cdots + q_m(x) = 0$$

has multiple solution in ζ :

$$\zeta_j(a) = \zeta_k(a) \quad (j \neq k)$$

(ii) A point $x = a$ is said to be a **virtual turning point** if $x = a$ is a x -component of a self-intersection point of the projection of bicharacteristic strip.



N. Honda, T. Kawai and Y. Takei,
Virtual turning points (Springer, 2015)

(iii) Let $x = a$ be a turning point of type (j, k) . Then a **Stokes curve** that emanates from a is the curve given by

$$\operatorname{Im} \int_a^x (\zeta_j(x) - \zeta_k(x)) dx = 0$$

Differential equations acting on the integral

For fixed q_0 case, we can systematically derive differential equations acting on $u(q_n)$ ($n = 2, 3, \dots$) by iterating the mapping relation in the inverse direction.

For $n = 2$

$$\left(\frac{d^2}{dq_2^2} - 2\eta(q_2 + 1) \frac{d}{dq_2} + \eta^2(q_2^2 + q_2 - q_0 + c) + \eta \right) u(q_2) = 0$$

For $n = 3$

$$\begin{aligned} & \left(\frac{d^4}{dq_3^4} - 4\eta(q_3 + 1) \frac{d^3}{dq_3^3} + \left((6q_3^2 + 10q_3 + 2c + 6)\eta^2 - 6\eta \right) \frac{d^2}{dq_3^2} \right. \\ & \quad + \left((-4q_3^3 - 8q_3^2 - 4cq_3 - 8q_3 - 4c - 3)\eta^3 + (12q_3 + 8)\eta^2 \right) \frac{d}{dq_3} \\ & \quad + \left((q_3^4 + 2q_3^3 + 2cq_3^2 + 3q_3^2 + 2cq_3 + q_3 + c^2 + 3c - q_0)\eta^4 \right. \\ & \quad \left. \left. + (-6q_3^2 - 7q_3 - 2c - 2)\eta^3 + 3\eta^2 \right) \right) u(q_3) = 0 \end{aligned}$$

Virtual turning points and new Stokes curves

— Multiple integral case —

Multiple integral

$$I(z; \eta) = \int \cdots \int_C \exp \left(\eta S(z; t) \right) dt_1 \cdots dt_p \quad (t = (t_1, \cdots, t_p))$$

Definition (Honda-Kawai-Takei)

- (i) A point z_0 is said to be an **ordinary turning point** of the system that $I(z; \eta)$ satisfies, if the following condition

$$S(z_0, t^{(j)}(z)) = S(z_0, t^{(k)}(z)) \quad (t^{(j)}(z) \neq t^{(k)}(z))$$

holds for $t^{(j)}(z)$ and $t^{(k)}(z)$.

- (ii) A point z_0 is said to be a **s-virtual turning point** of the system that $I(z; \eta)$ satisfies, if there exist t and $t' (\neq t)$ for which the following conditions are satisfied

$$S(z_0, t) = S(z_0, t')$$

$$(\text{grad}_t S)(z_0, t) = (\text{grad}_{t'} S)(z_0, t') = 0$$

Virtual turning points and new Stokes curves

— Multiple integral case —

(iii) Curves emanating from an ordinary (resp. virtual) turning point z_0 satisfying

$$\operatorname{Im} S(z_0, t^{(j)}(z)) = \operatorname{Im} S(z_0, t^{(k)}(z))$$

are called **ordinary** (resp. **new**) Stokes curves.

Virtual turning points and new Stokes curves

— Multiple integral case —

From the mapping relation,

$$F : (q_{i+1} - q_i) - (q_i - q_{i-1}) = -V'(q_i)$$

we can write down q_{i+1} ($1 \leq i \leq n-1$) as a polynomial of (q_0, q_1) . In particular, we find

$$q_n = q_1^{2^n-1} + Q_n(q_0, q_1)$$

where Q_n is a polynomial of (q_0, q_1) whose degree in q_1 is less than 2^{n-1} . Thus, q_1 satisfies an algebraic equation whose coefficients depend only on (q_0, q_1) , and we locally find 2^{n-1} solutions $q_1^{(j)}$ ($j = 1, 2, \dots, 2^{n-1}$).

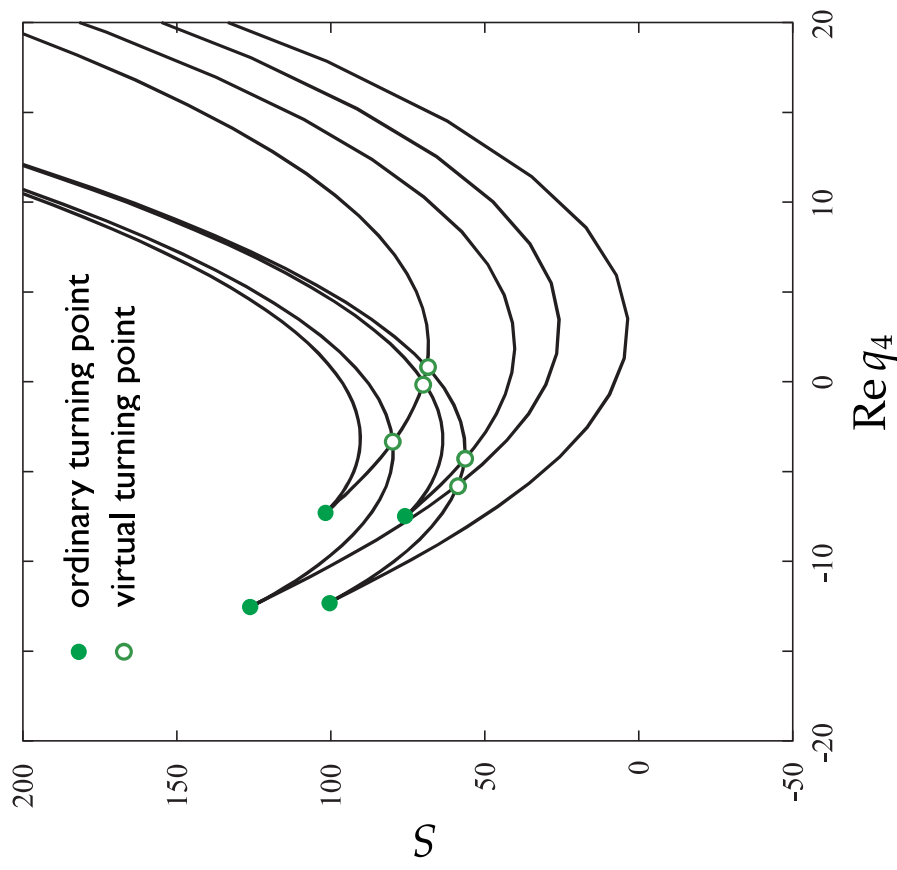
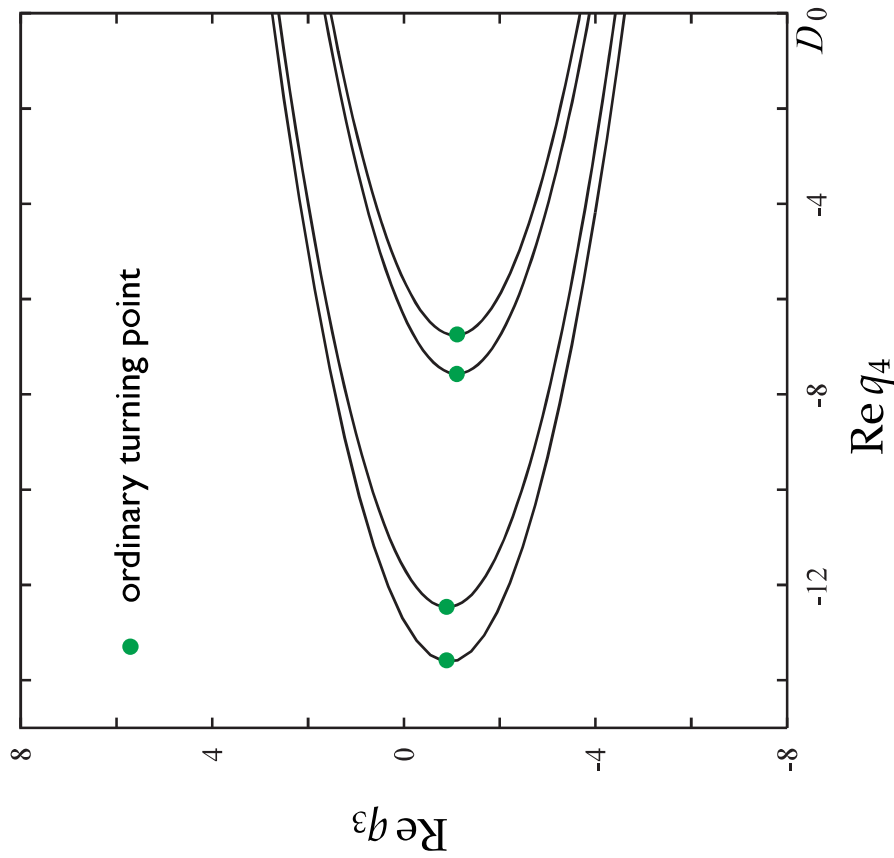
By using $q_1^{(j)}$ given above, we find a point (q_0, q_1) is a **s-virtual point** if

$$\begin{aligned} & S(q_0, q_1^{(j)}(q_0, q_n), q_2(q_0, q_1^{(j)}(q_0, q_1)), \dots, q_{n-1}(q_0, q_1^{(j)}(q_0, q_1)), q_n) \\ &= S(q_0, q_1^{(k)}(q_0, q_n), q_2(q_0, q_1^{(k)}(q_0, q_1)), \dots, q_{n-1}(q_0, q_1^{(k)}(q_0, q_1)), q_n) \end{aligned}$$

holds for ($j \neq k$).

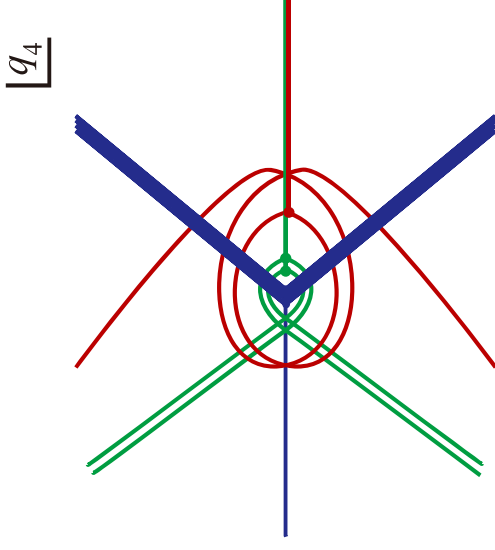
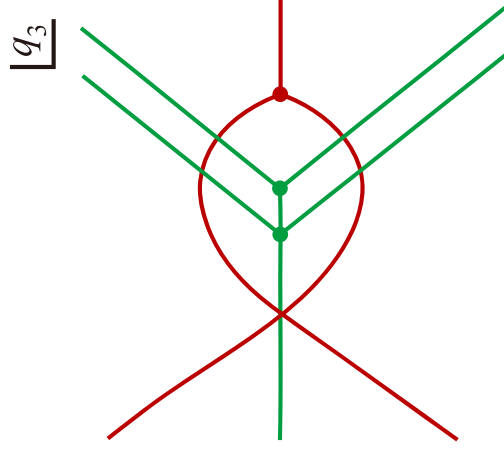
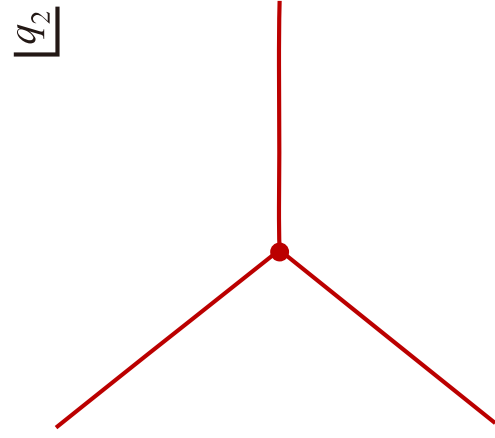
Ordinary turning points and virtual turning points

For a fixed q_0 , the action $S(q_0, q_1, q_1(q_0, q_1), \dots, q_n(q_0, q_1))$ can be regarded as a function of q_1 , so the q_1 play the role of the time in the Hamilton-Jacobi equation.



Time evolution of Stokes geometry for the quantum Hénon map

Stokes geometry (ordinary Stokes curves only)

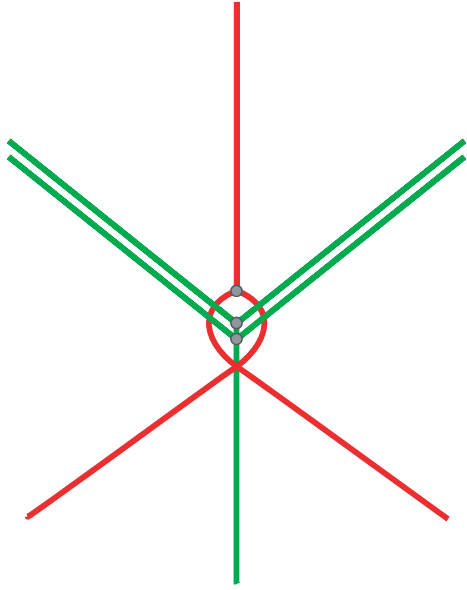
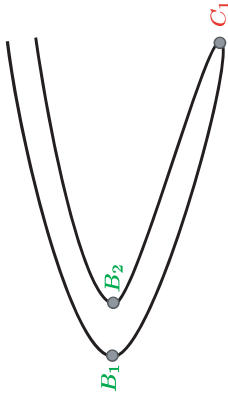


2-step once folding vs 1-step three times folding

2-step once folding

$$u(q_0, q_3) = \int_{-\infty}^{\infty} \int_{-\infty}^{\infty} dq_1 dq_2 \exp\left[\eta S(q_0, q_1, q_2, q_3)\right]$$

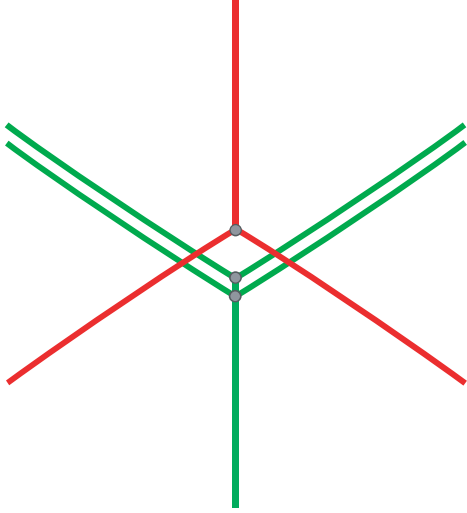
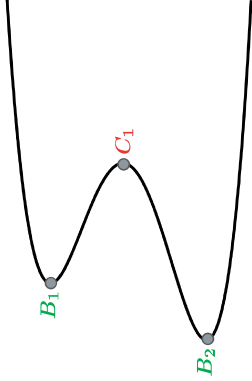
$$S(q_0, q_1, q_2, q_3) = \sum_{j=1}^3 \frac{1}{2} (q_j - q_{j-1})^2 + \sum_{j=1}^2 \left(\frac{1}{3} q_j^3 + c q_j\right)$$



1-step three times folding

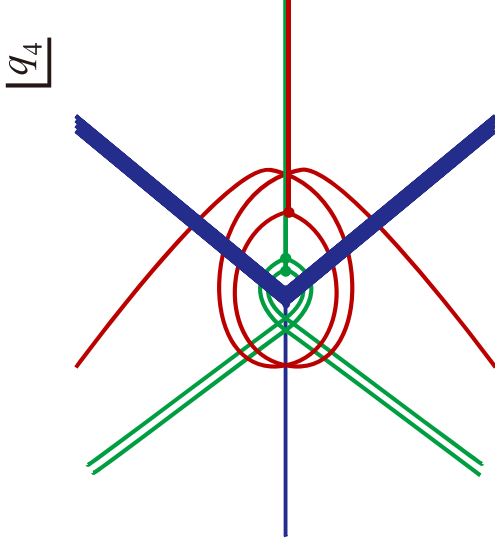
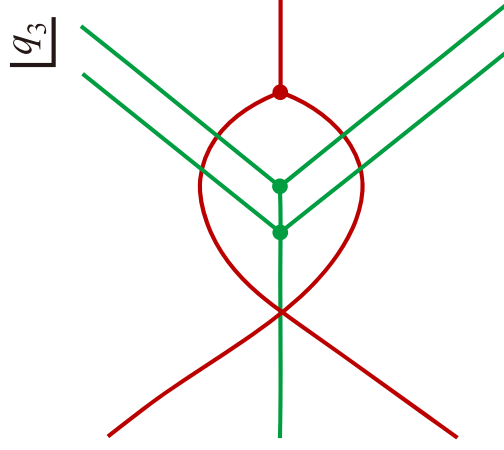
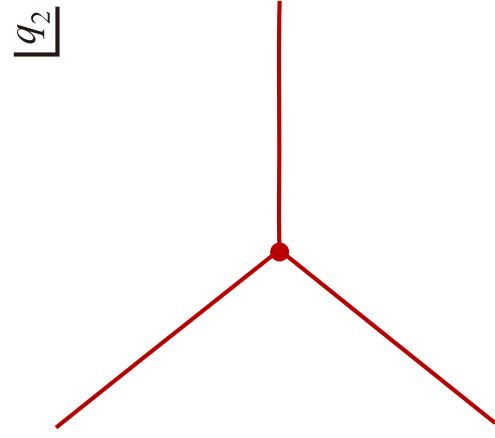
$$u(q_0, q_2) = \int_{-\infty}^{\infty} dq_1 \exp\left[\eta S(q_0, q_1, q_2)\right]$$

$$S(q_0, q_1, q_2) = \sum_{j=1}^2 \frac{1}{2} (q_j - q_{j-1})^2 + \sum_{j=1}^5 c_j q_j^j$$

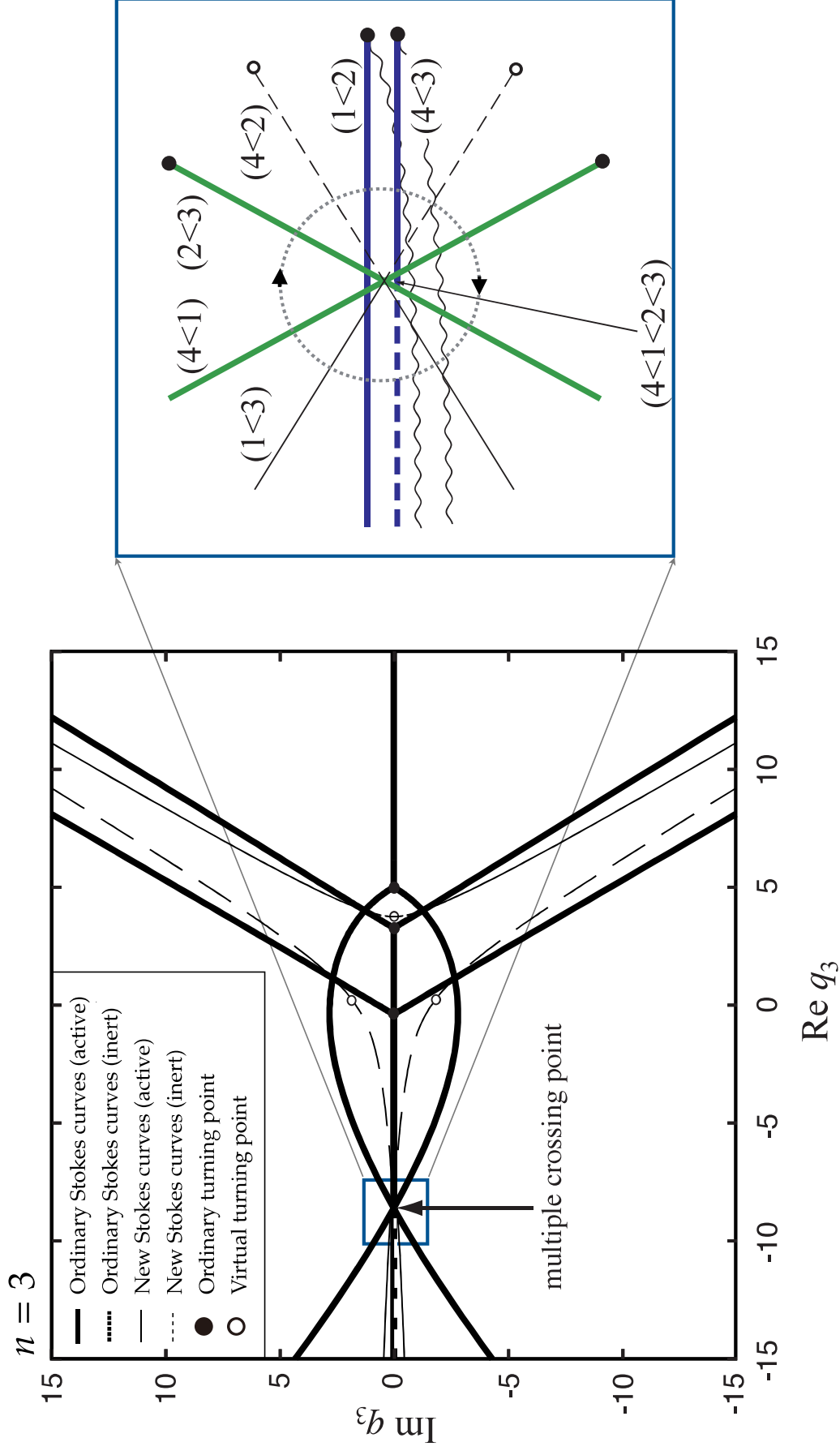


Time evolution of Stokes geometry for the quantum Hénon map

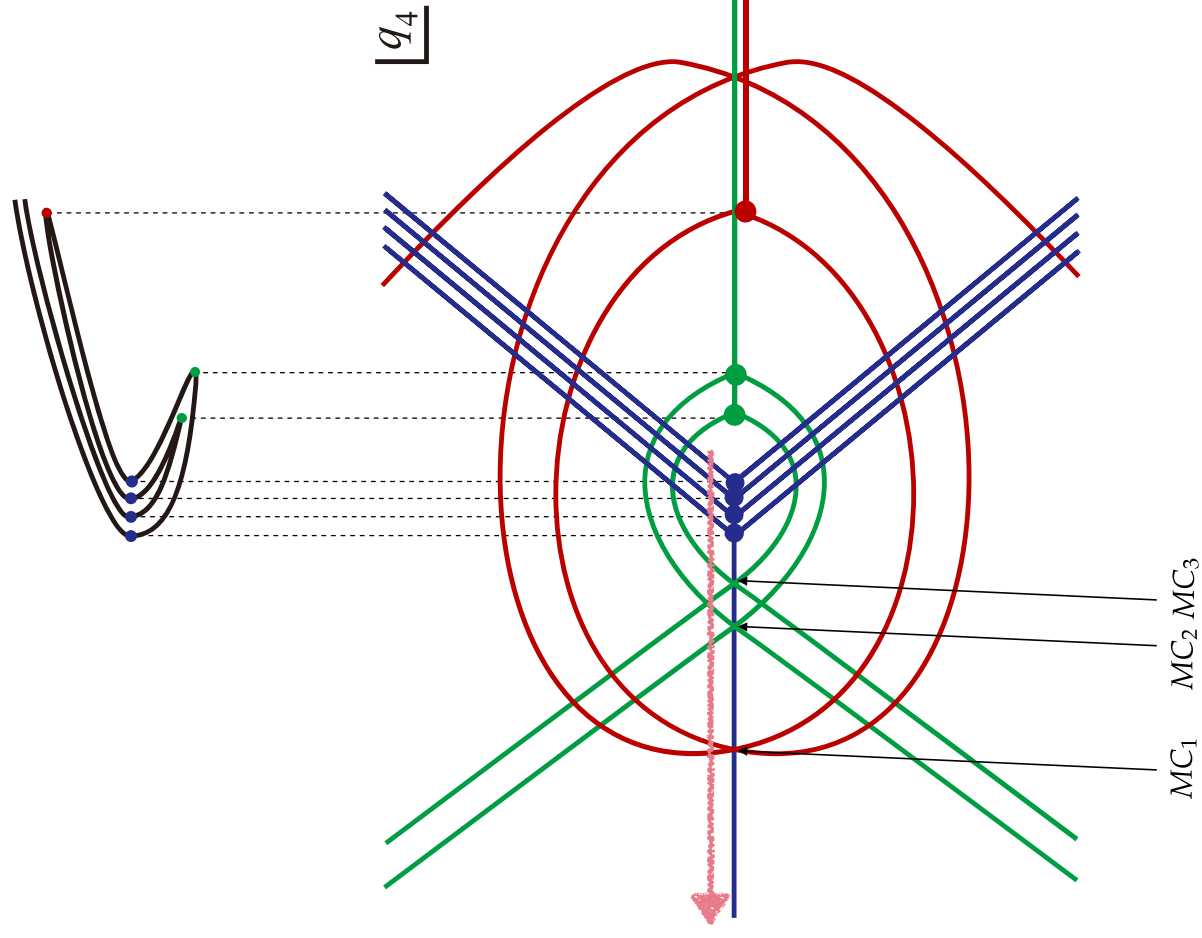
Stokes geometry (ordinary Stokes curves only)



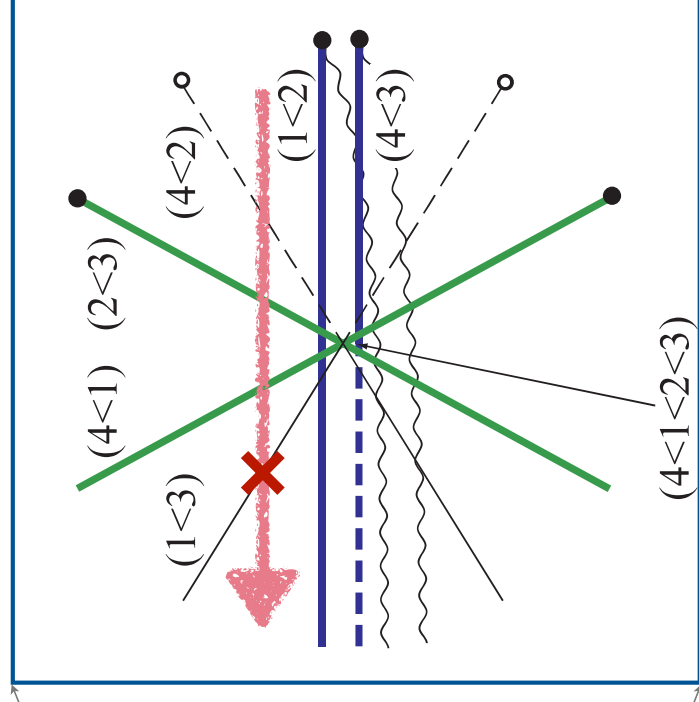
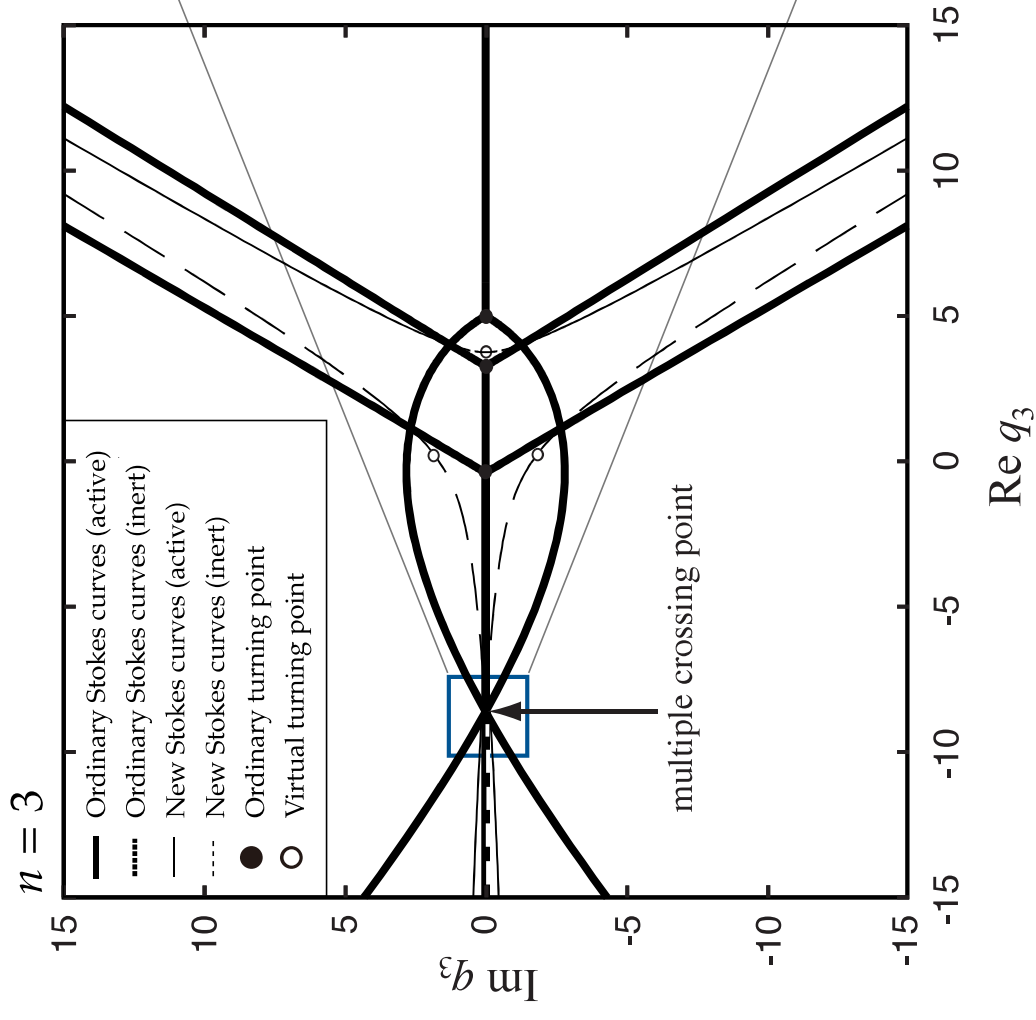
Multiple crossing point



Sequence of multiple crossing points on the real axis

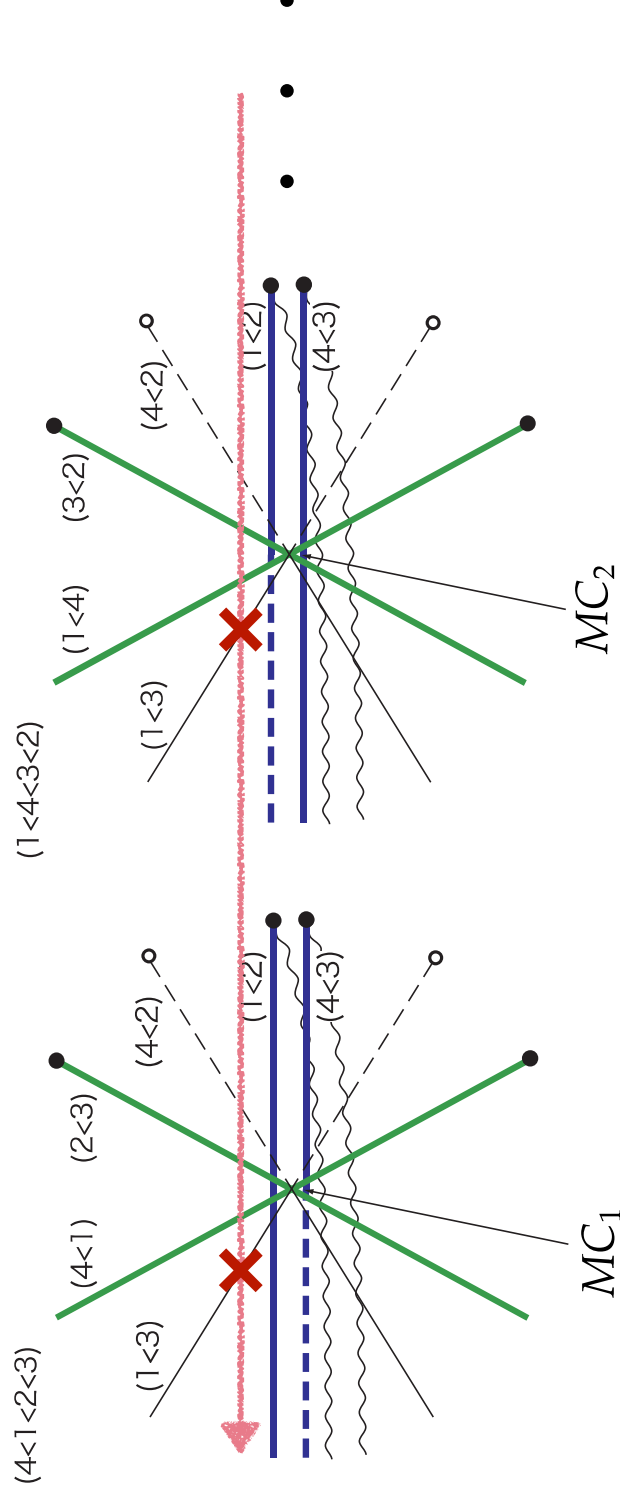


Active new Stokes curves crossing the real axis



Active new Stokes curves crossing the real axis

- Let MC_1 be the leftmost multiple crossing point on the $\text{Re}q_n$ -axis.
- In order to realize the situation where the Stoke phenomenon occurs on the new Stokes curve ($1 < 3$), the solution u_3 should exist at MC_1 .
- However, u_3 is exponentially growing as $\text{Re}q_n \rightarrow -\infty$, so u_3 cannot exist at MC_1 , which means that the new Stokes curve ($1 < 3$) does not play any role.
- The same argument applies to the next leftmost multiple crossing point MC_2 and so on.



Summary

We have examined the role of the new Stokes curves in the following two situations of physical origin.

1. Feynman propagator for the discrete dynamical systems

Saddle point solutions associated with the connection on active new Stokes curves are dropped due to the boundary condition, the effect of new Stokes curves does not appear explicitly.

Outline

In Stokes geometry for high-order differential equations, new Stokes curves appear in addition to the conventional Stokes curves. New Stokes curves must also be considered when performing saddle point evaluation of integrals involving more than two saddle points. It would be fascinating to identify situations where these new objects play a significant role and predict new phenomena in physics. Here we explore this possibility through the following two examples:

1. Feynman propagator for the discrete dynamical systems
2. Multi-state non-adiabatic transition

Models for nonadiabatic transition (two levels)

Two-state nonadiabatic transition model

$$i\hbar \frac{d}{dt} \begin{pmatrix} \psi^{(1)} \\ \psi^{(2)} \end{pmatrix} = \left[\begin{pmatrix} \rho_1(t) & 0 \\ 0 & \rho_2(t) \end{pmatrix} + \begin{pmatrix} 0 & c_{12} \\ c_{12}^* & 0 \end{pmatrix} \right] \begin{pmatrix} \psi^{(1)} \\ \psi^{(2)} \end{pmatrix} \quad (\hbar: \text{small parameter, } c_{ij} = \text{const})$$

Linear $\rho_j(t)$: Landau, Zener, Stückelberg, Mayonara

Nonlinear $\rho_j(t)$: ...

Non-Adiabatic Crossing of Energy Levels.

By CLARENCE ZENER, National Research Fellow of U.S.A.

(Communicated by R. H. Fowler, F.R.S.—Received July 19, 1932.)

1. *Introduction.*

The crossing of energy levels has been a matter of considerable discussion.* The essential features may be illustrated in the crossing of a polar and homopolar state of a molecule.

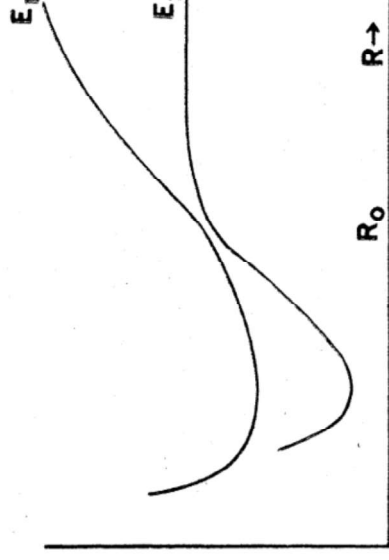


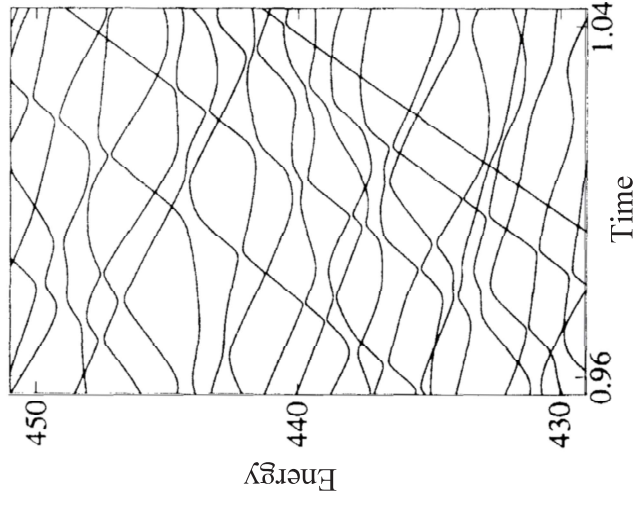
FIG. 1.—Crossing of polar and homopolar states.

Models for nonadiabatic transition (multiple levels)

Multi-state nonadiabatic transition model

$$i\hbar \frac{d}{dt} \begin{pmatrix} \psi^{(1)} \\ \psi^{(2)} \\ \vdots \\ \psi^{(N)} \end{pmatrix} = \left[\begin{pmatrix} \rho_1(t) & 0 & \dots & 0 \\ 0 & \rho_2(t) & \dots & 0 \\ \vdots & \vdots & \ddots & \vdots \\ 0 & 0 & \dots & \rho_N(t) \end{pmatrix} + \begin{pmatrix} 0 & c_{12} & \dots & c_{1N} \\ \overline{c_{12}} & 0 & \dots & c_{2N} \\ \vdots & \vdots & \ddots & \vdots \\ \overline{c_{1N}} & \overline{c_{2N}} & \dots & 0 \end{pmatrix} \right] \begin{pmatrix} \psi^{(1)} \\ \psi^{(2)} \\ \vdots \\ \psi^{(N)} \end{pmatrix}$$

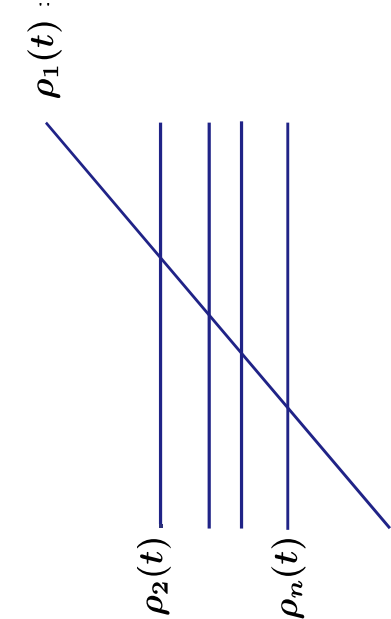
Linear $\rho_j(t)$: Carroll-Hioe, Demkov, Osherov, Ostrovsky, Sinitsyn, Brundobler-Elser, ...
 Nonlinear $\rho_j(t)$: Sinitsyn, Joye, ...



Solvable models

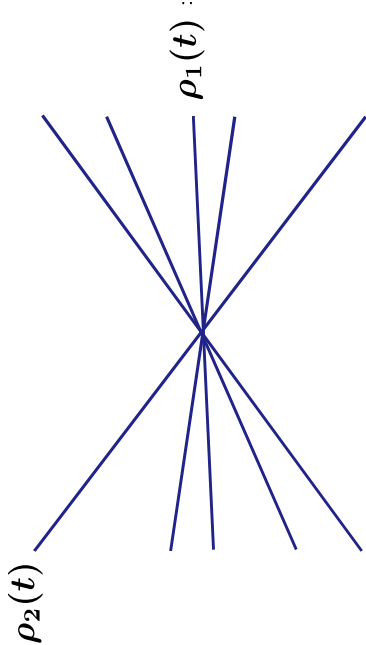
Equal-slope model (Demkov-Osherov, 1967)

$$\rho_1(t) = \alpha t, \quad \rho_2(t) = \beta_2, \dots, \rho_n(t) = \beta_n$$

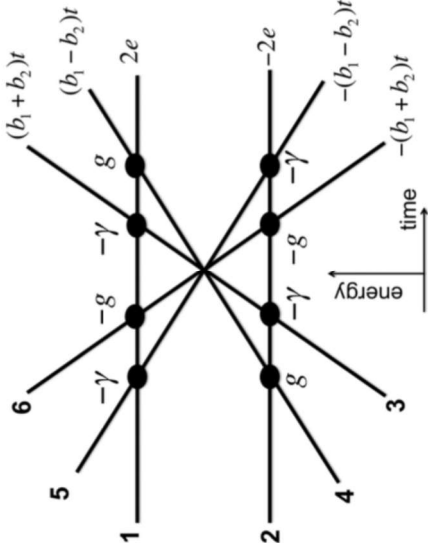


Bowtie model (Carroll-Hioe, 1985)

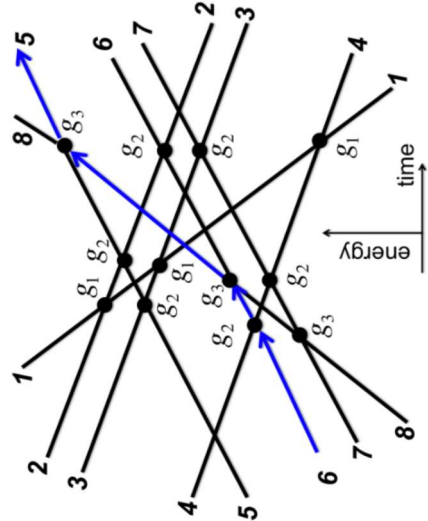
$$\rho_1(t) = 0, \quad \rho_2(t) = \alpha_2 t, \dots, \rho_n(t) = \alpha_n t$$



Generalizations (Demkov, Ostrovsky, Shytov, Patra-Yuzbashyan, Sinitsyn, ...)



(Sinitsyn, Lin and Chernyak, PRA 95, 012140 (2017))



(Sinitsyn, Lin and Chernyak, PRA 93, 063859 (2016))

Exact WKB analysis of non-adiabatic transition probabilities for three levels

Three-state nonadiabatic transition model (Aoki-Kawai-Takei)

$$i\frac{d}{dt}\begin{pmatrix} \psi^{(1)} \\ \psi^{(2)} \\ \psi^{(3)} \end{pmatrix} = \eta \left[\begin{pmatrix} \rho_1(t) & 0 & 0 \\ 0 & \rho_2(t) & 0 \\ 0 & 0 & \rho_3(t) \end{pmatrix} + \eta^{\frac{1}{2}} \begin{pmatrix} 0 & c_{12} & c_{13} \\ \frac{c_{12}}{c_{13}} & 0 & c_{23} \\ \frac{c_{13}}{c_{23}} & \frac{c_{23}}{c_{13}} & 0 \end{pmatrix} \right] \begin{pmatrix} \psi^{(1)} \\ \psi^{(2)} \\ \psi^{(3)} \end{pmatrix} \quad (\eta = 1/\hbar)$$

$\rho_j(t)$ ($j = 1, 2, 3$): polynomial functions of t

Exact WKB analysis of non-adiabatic transition probabilities for three levels

Three-state nonadiabatic transition model (Aoki-Kawai-Takei)

$$i \frac{d}{dt} \begin{pmatrix} \psi^{(1)} \\ \psi^{(2)} \\ \psi^{(3)} \end{pmatrix} = \eta \left[\begin{pmatrix} \rho_1(t) & 0 & 0 \\ 0 & \rho_2(t) & 0 \\ 0 & 0 & \rho_3(t) \end{pmatrix} + \eta^{\frac{1}{2}} \begin{pmatrix} 0 & c_{12} & c_{13} \\ \frac{c_{12}}{c_{13}} & 0 & c_{23} \\ \frac{c_{13}}{c_{23}} & \frac{c_{23}}{c_{13}} & 0 \end{pmatrix} \right] \begin{pmatrix} \psi^{(1)} \\ \psi^{(2)} \\ \psi^{(3)} \end{pmatrix} \quad (\eta = 1/\hbar)$$

$\rho_j(t)$ ($j = 1, 2, 3$): polynomial functions of t

Concrete recipe to provide S -matrix based on the exact WKB method

- 1) local WKB solution
- 2) connection formula passing through Stokes curves
- 3) locating turning points (ordinary+virtual) and drawing Stokes curves (ordinary+new)
- 4) explicit expression for S -matrix

Exact WKB analysis of non-adiabatic transition probabilities for three levels

1) local WKB solution

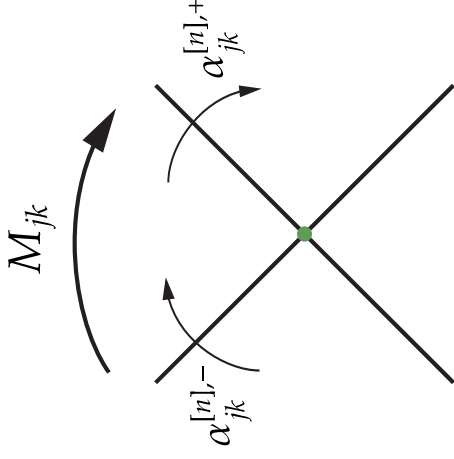
$$\psi^{(i)} = \exp \left[\frac{\eta}{i} \int_{t_0}^t \rho_j(t) dt + \frac{1}{i} \int_{t_0}^t \left(\frac{|c_{jk}|^2}{\rho_j(t) - \rho_k(t)} + \frac{|c_{j\ell}|^2}{\rho_j(t) - \rho_\ell(t)} \right) dt \right] \left(e^{(i)} + O(\eta^{-1/2}) \right)$$

2) Connection formula passing through Stokes curves

$$(\psi^{(1)}, \psi^{(2)}, \psi^{(3)}) \longmapsto (\psi^{(1)}, \psi^{(2)}, \psi^{(3)}) M^{[n]}$$

where

$$M_{12} = \begin{pmatrix} 1 + \alpha_{12}^- \alpha_{12}^+ & -\alpha_{12}^+ & 0 \\ -\alpha_{12}^- & 1 & 0 \\ 0 & 0 & 1 \end{pmatrix} \quad M_{23} = \begin{pmatrix} 1 & 0 & 0 \\ 0 & 1 + \alpha_{23}^- \alpha_{23}^+ & -\alpha_{23}^+ \\ 0 & -\alpha_{23}^- & 1 \end{pmatrix} \quad M_{13} = \begin{pmatrix} 1 + \alpha_{13}^- \alpha_{13}^+ & 0 & -\alpha_{13}^+ \\ 0 & -\alpha_{13}^- & 0 \\ -\alpha_{13}^- & 0 & 1 \end{pmatrix}$$



Exact WKB analysis of non-adiabatic transition probabilities for three levels

Stokes coefficients are given as

$$\alpha_{jk}^{[n],\pm} = c_{jk}^{\pm} \frac{i\sqrt{2\pi}}{\Gamma(1 \pm \kappa_{jk}^{[n]})} (e^{\pm i\pi/2} \lambda_{jk}^{[n]})^{-1/2} (2\eta)^{\kappa_{jk}^{[n]}} e^{1/2 \mp 1) i\pi/2 \kappa_{jk}^{[n]}} (\beta_{jk}^{[n]})^{\pm 1}$$

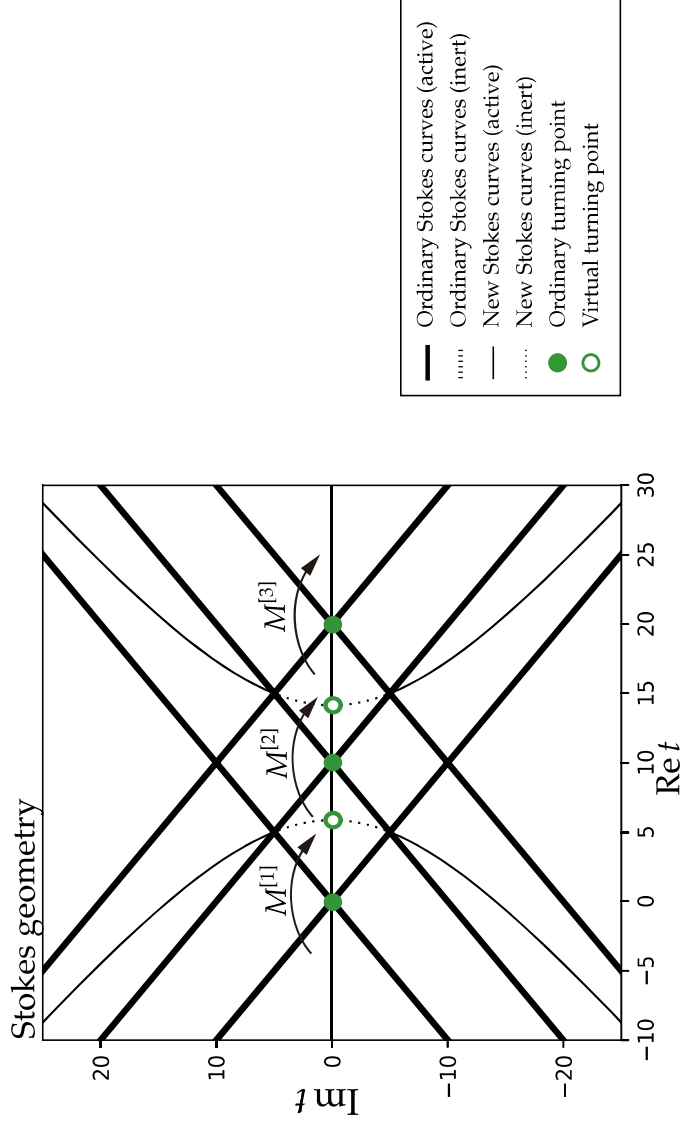
and

$$c_{jk}^{+} = c_{jk}, \quad \overline{c_{jk}^{-}} = \overline{c_{jk}}, \quad \kappa_{jk}^{[n]} = \frac{i|c_{jk}|^2}{\lambda_{jk}^{[n]}}$$

$\beta_{jk}^{[n]}$ is computed by comparing the WKB solutions reduced to the 2-level systems.

Exact WKB analysis of non-adiabatic transition probabilities for three levels

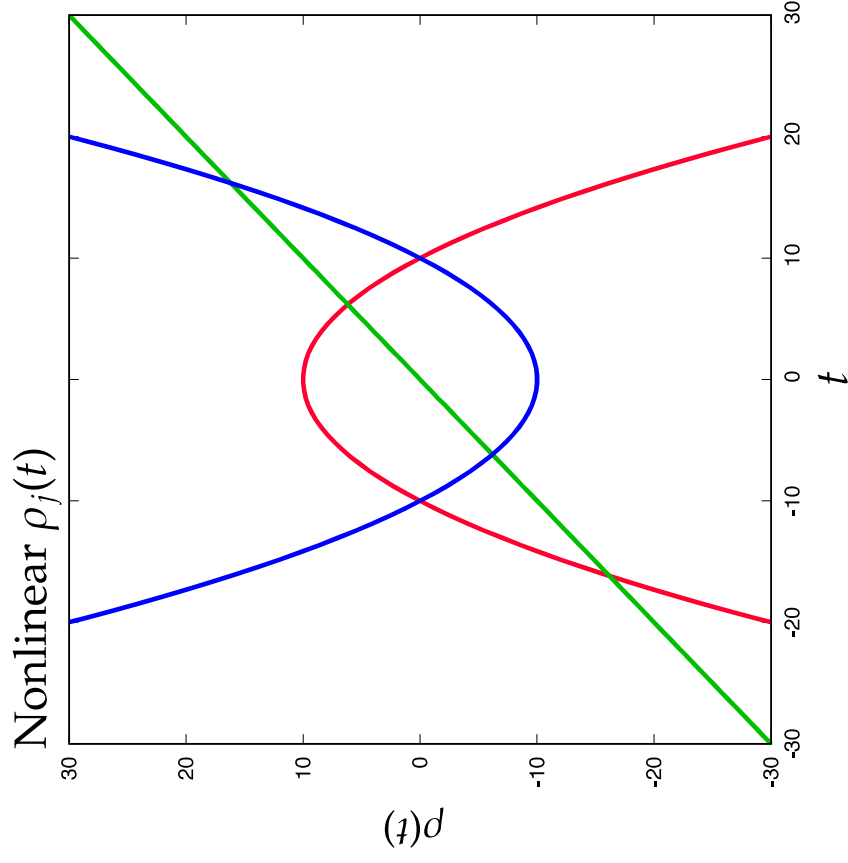
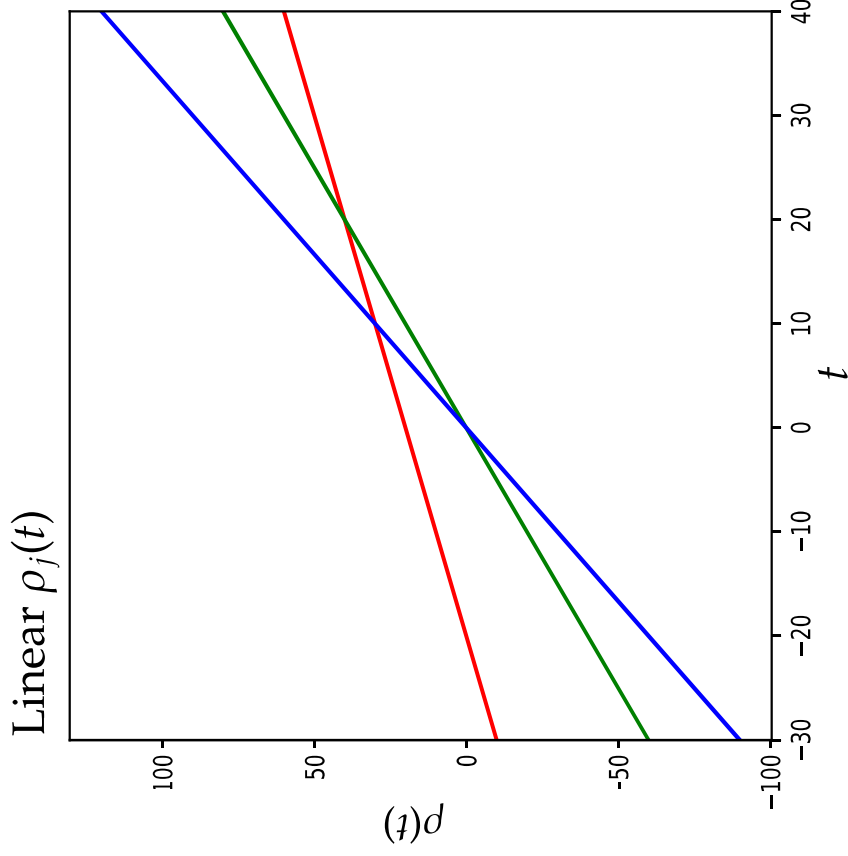
3) locating turning points (ordinary+virtual) and drawing Stokes curves (ordinary+new)



4) Explicit expression for S-matrix

$$S = \begin{pmatrix} N_1^+ & 0 & 0 \\ 0 & N_2^+ & 0 \\ 0 & 0 & N_3^+ \end{pmatrix} M^{[n]} M^{[n-1]} \dots M^{[1]} \begin{pmatrix} N_1^- & 0 & 0 \\ 0 & N_2^- & 0 \\ 0 & 0 & N_3^- \end{pmatrix}$$

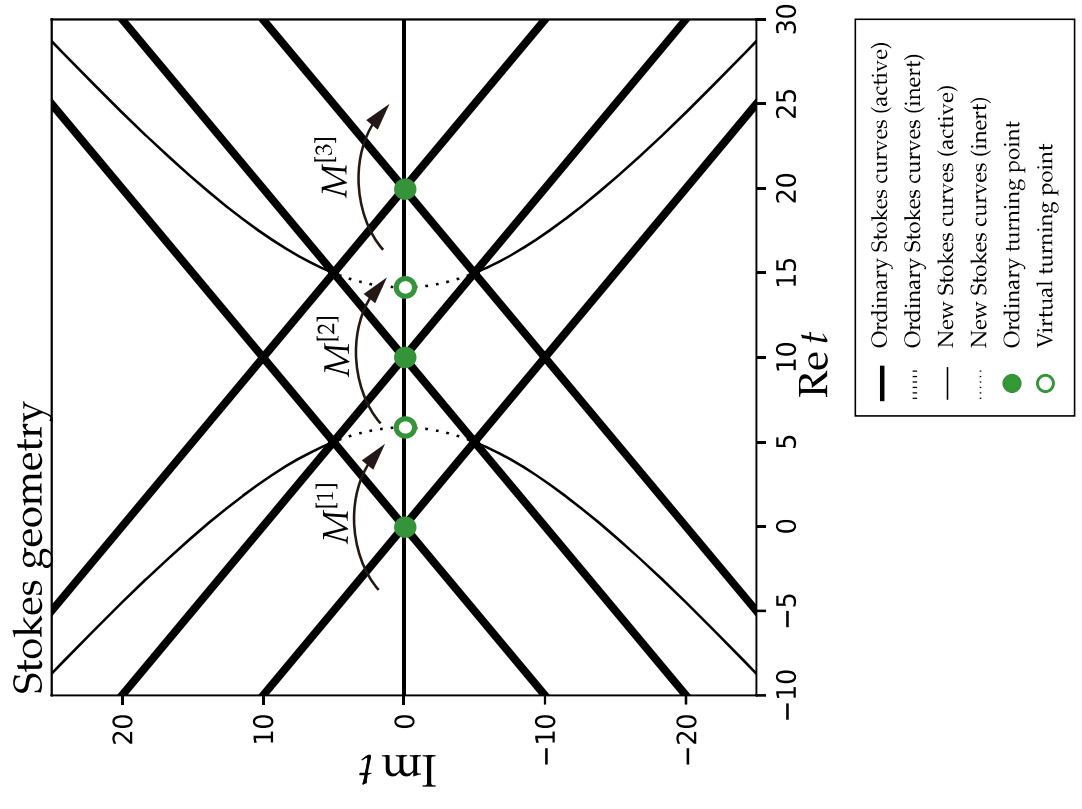
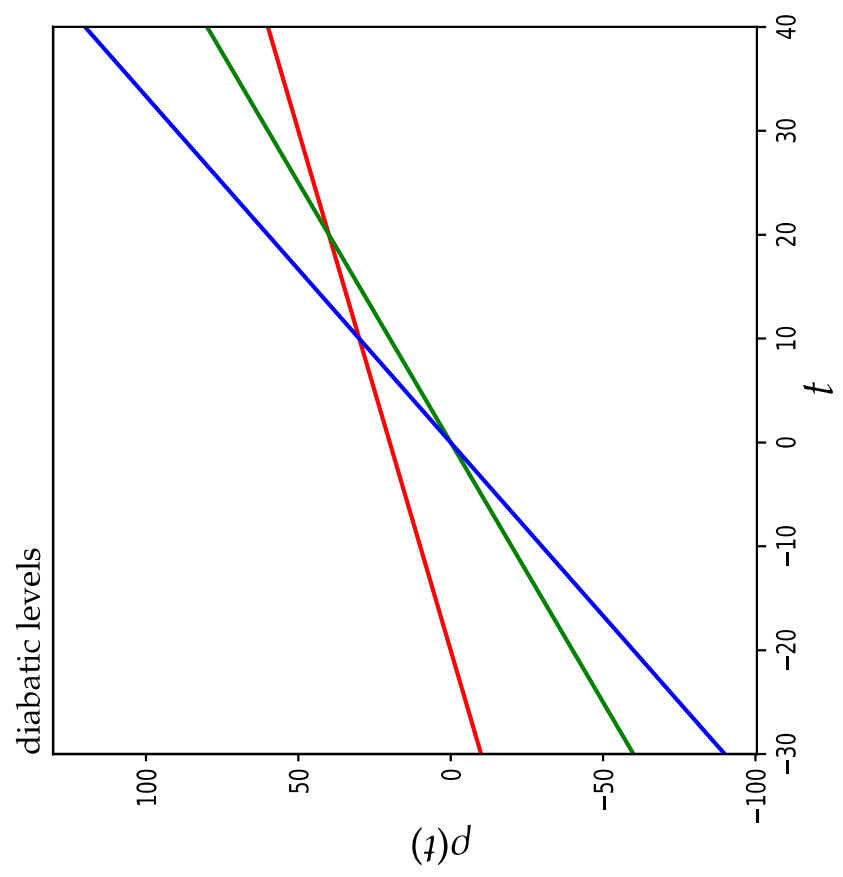
Numerical verification of the exact WKB prediction



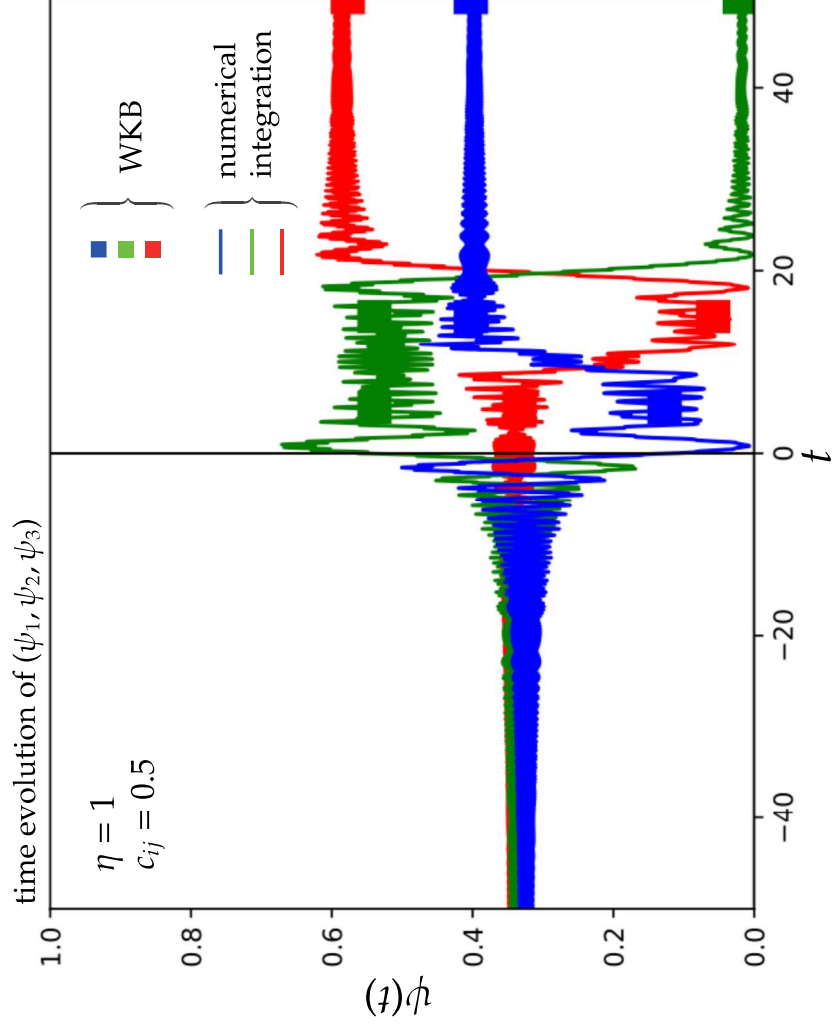
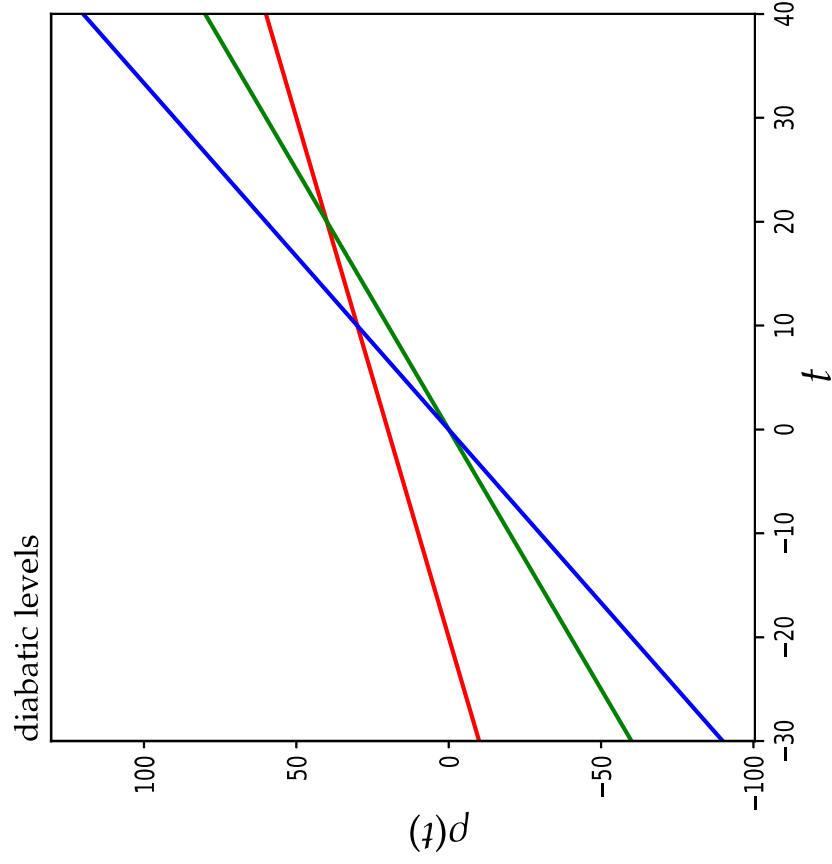
Proposition (Aoki-Kawai-Takei)

If $(\rho_1(t) - \rho_2(t))(\rho_2(t) - \rho_3(t))(\rho_3(t) - \rho_1(t)) = 0$ has only real and simple zeros, then a new Stokes curve emanating from a non-real virtual turning point never meets with the real axis.

Numerical verification of the exact WKB prediction (Linear case)

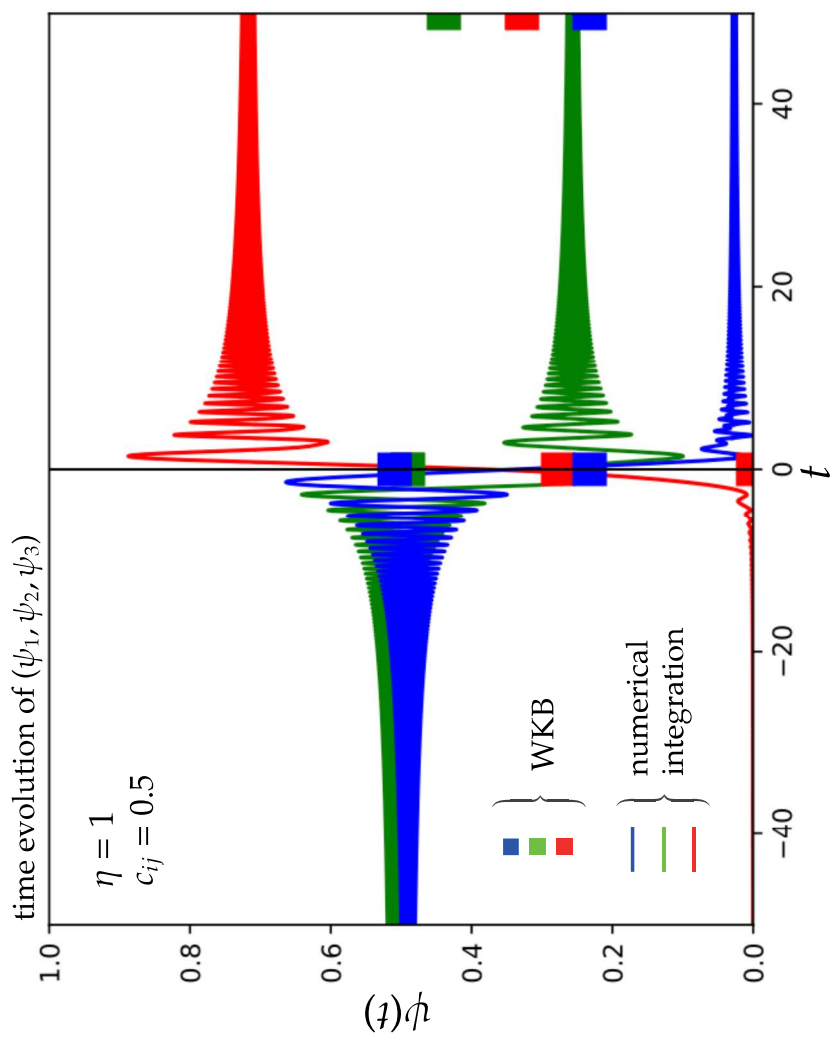
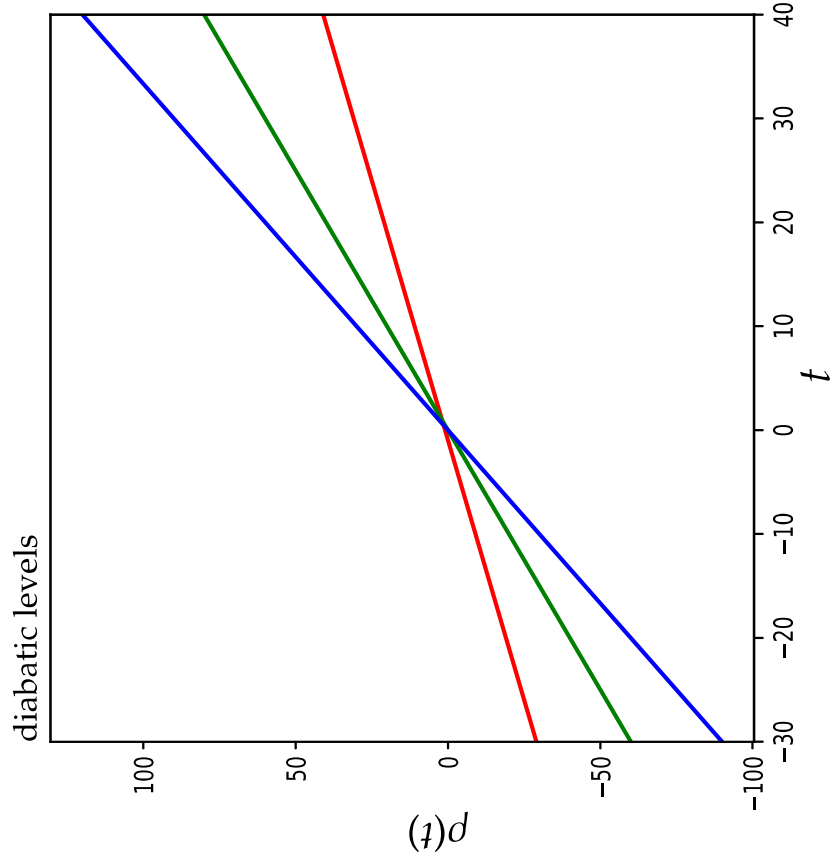


Coalescing of turning points



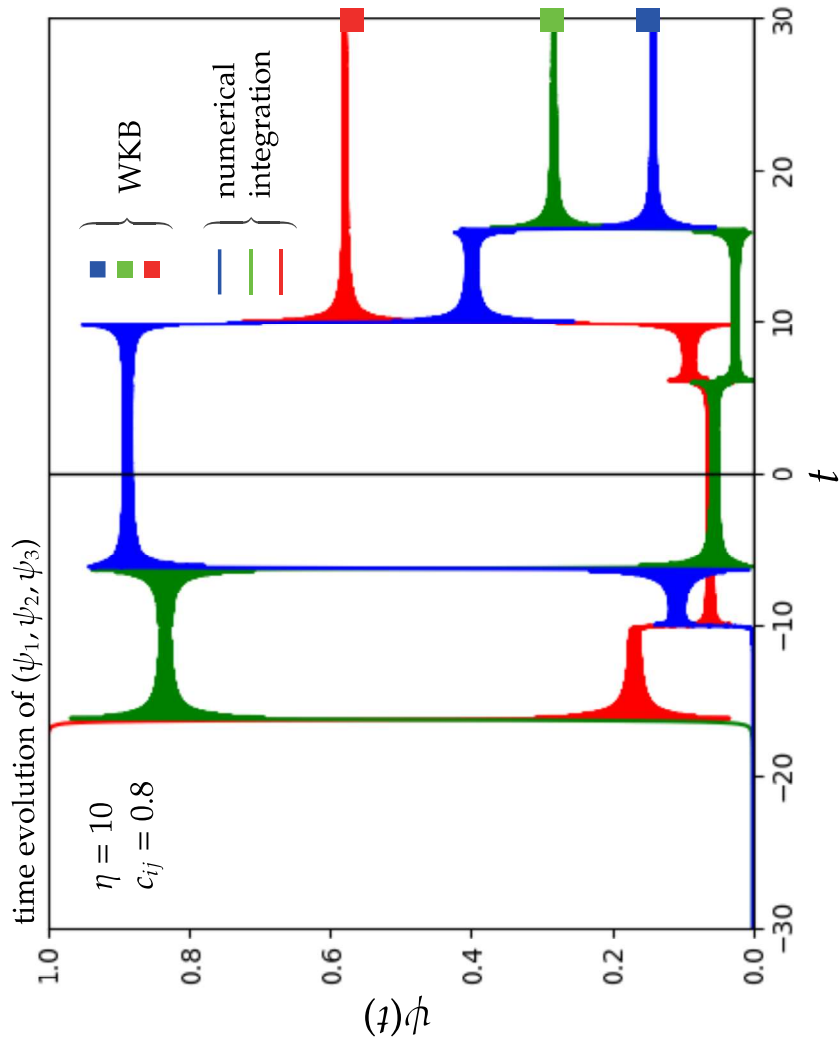
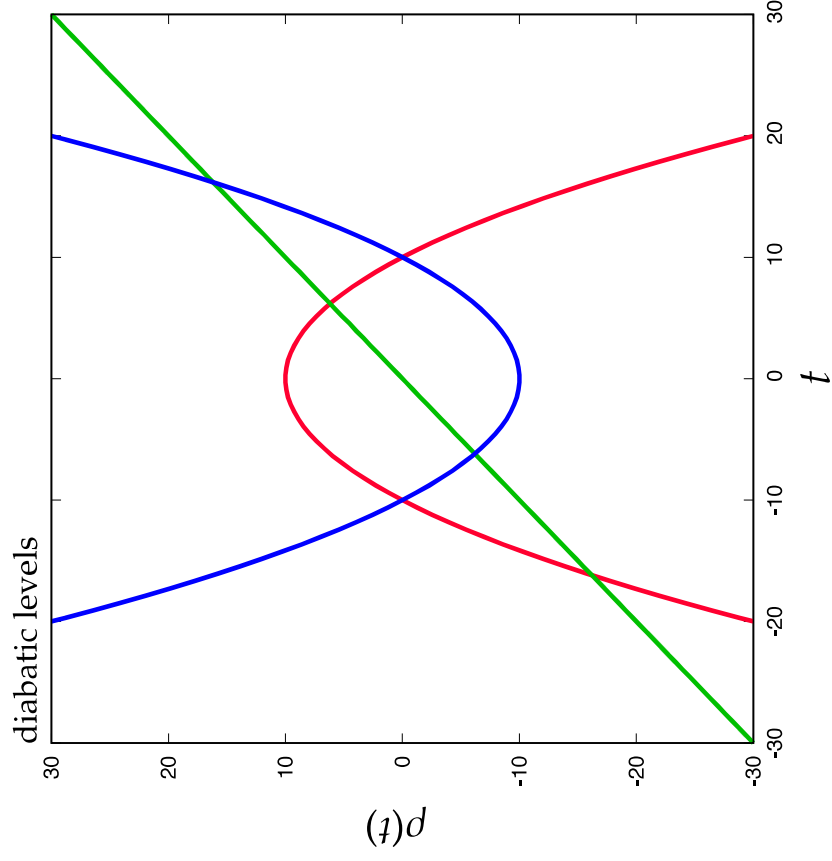
works well if turning points are well separated even though $\eta = 1$.

Coalescing of turning points



does not work if turning points are not well separated

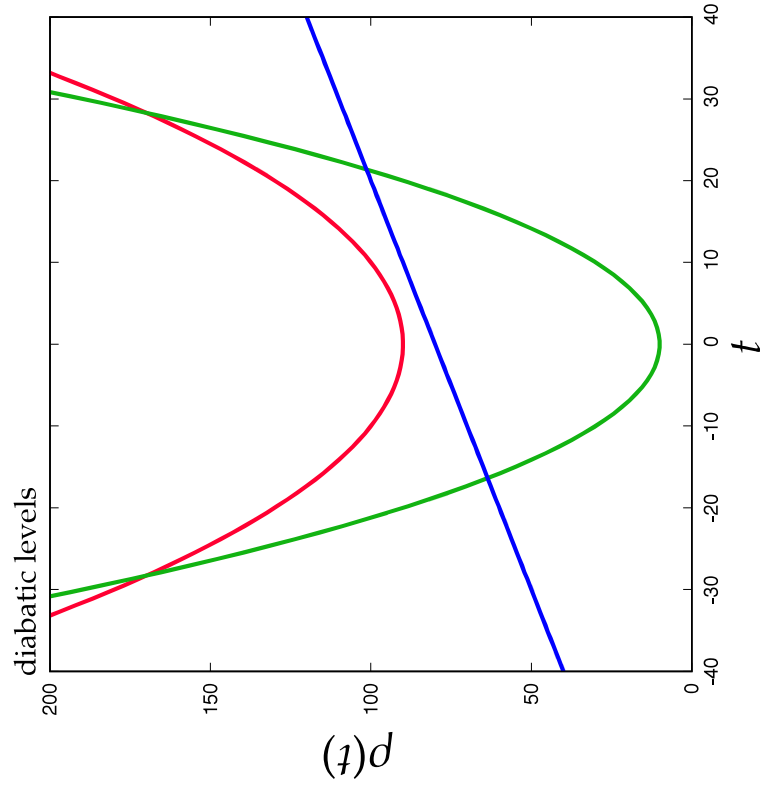
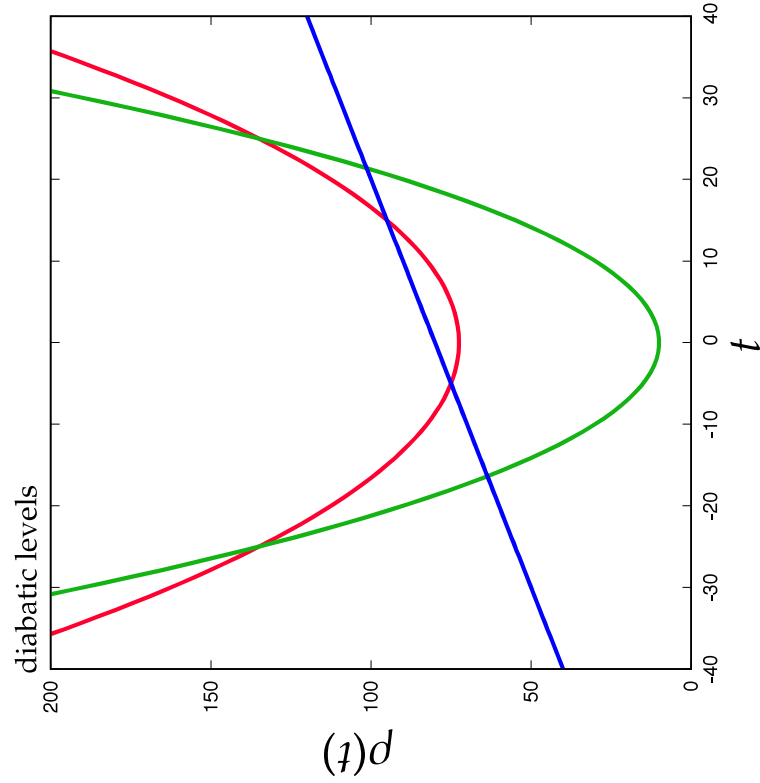
Numerical verification of the exact WKB prediction (Nonlinear case)



works well if turning points are well separated
even though diabatic energies are nonlinear.

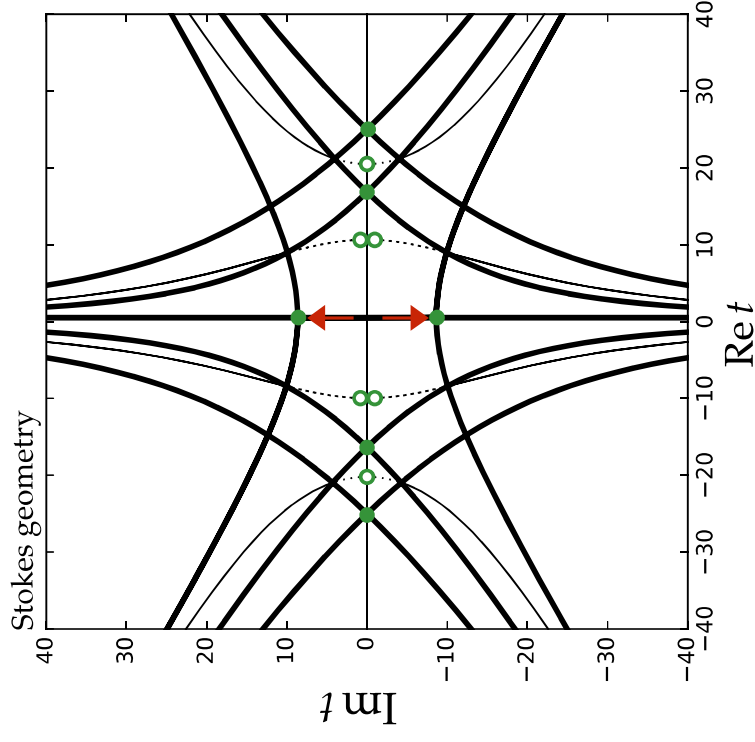
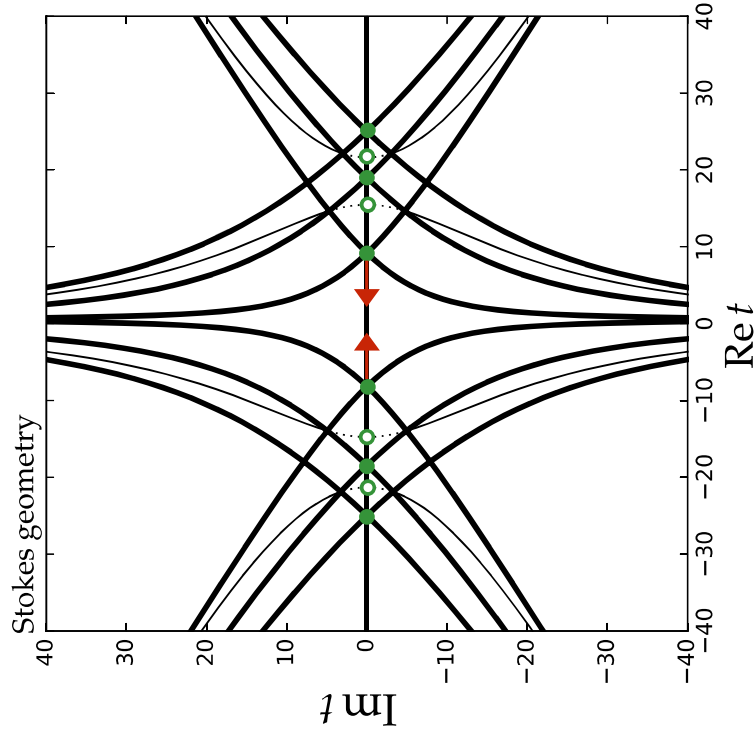
Bifurcation of the Stokes geometry

With the change of a parameter, some of ordinary turning points on the real axis degenerate and form a complex conjugate pair.



Bifurcation of the Stokes geometry

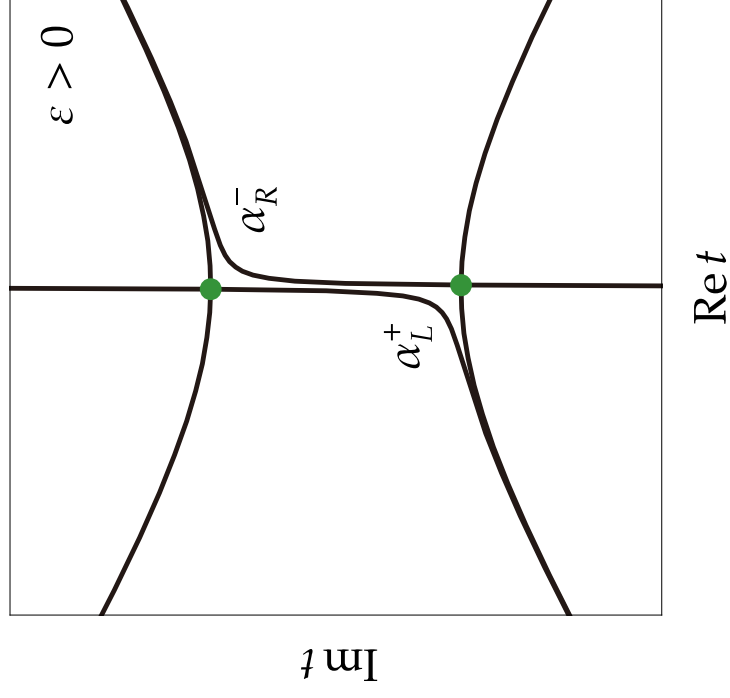
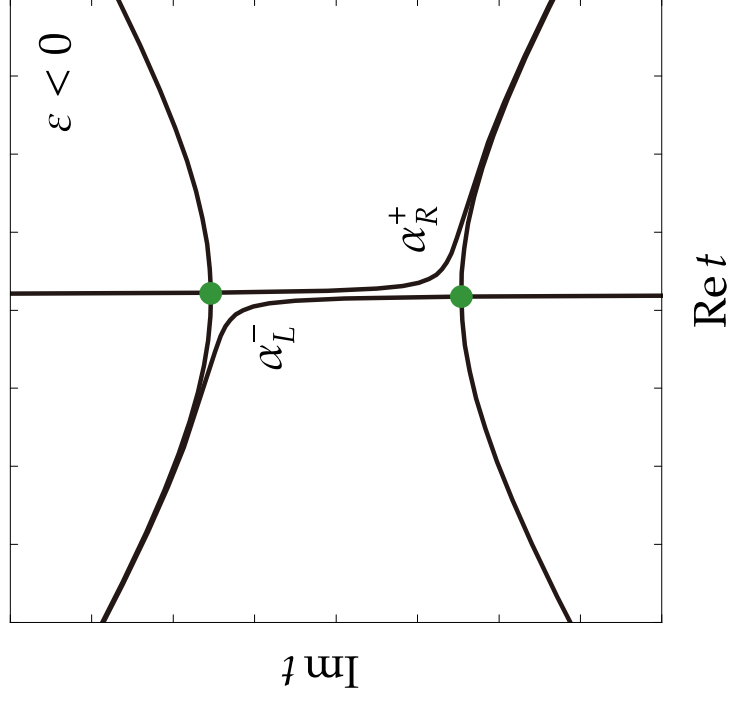
With the change of a parameter, some of ordinary turning points on the real axis degenerate and form a complex conjugate pair.



Connection across the degenerated Stokes curve

After the bifurcation, turning points are connected by a Stokes curve.

To resolve degeneracy, add an imaginary component $i\varepsilon$ to a parameter.



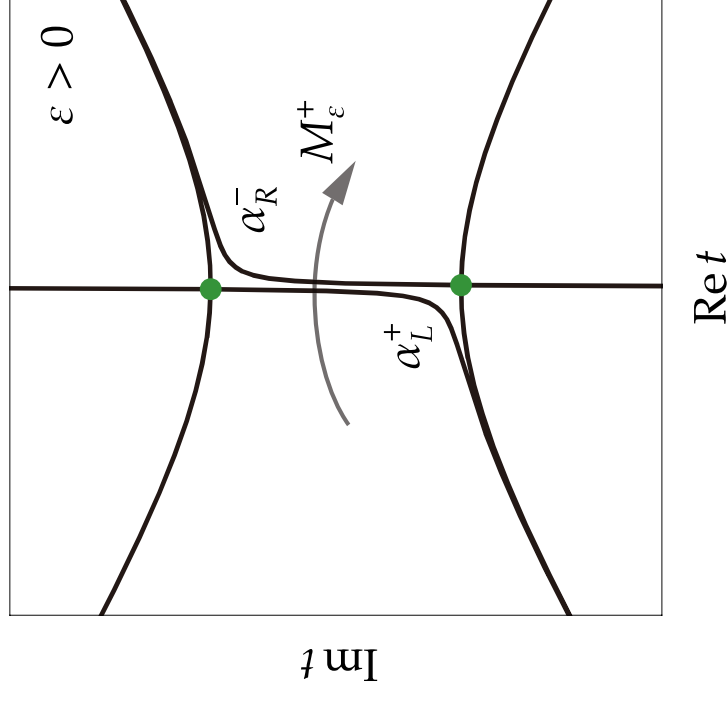
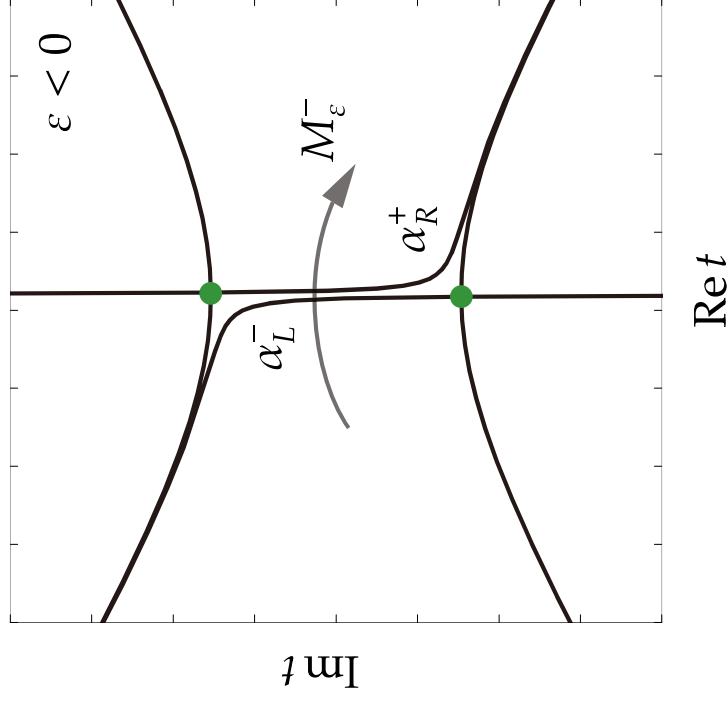
Connection across the degenerated Stokes curve

Connection across Stokes curves

$$\left(\psi^{(1)}, \psi^{(2)}\right) \longmapsto \left(\psi^{(1)}, \psi^{(2)}\right) M_{\varepsilon}^{\pm}$$

where

$$M_{\varepsilon}^{-} = \begin{pmatrix} 1 - \alpha_L^{-} \alpha_R^{+} & -\alpha_L^{-} \\ \alpha_R^{+} & 1 \end{pmatrix} \quad M_{\varepsilon}^{+} = \begin{pmatrix} 1 & -\alpha_L^{+} \\ \alpha_R^{-} & 1 - \alpha_L^{+} \alpha_R^{-} \end{pmatrix}$$

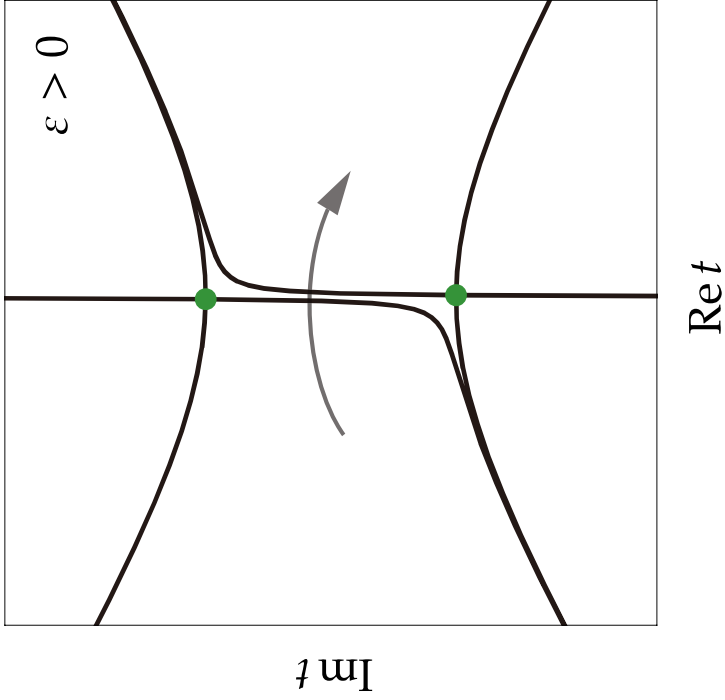
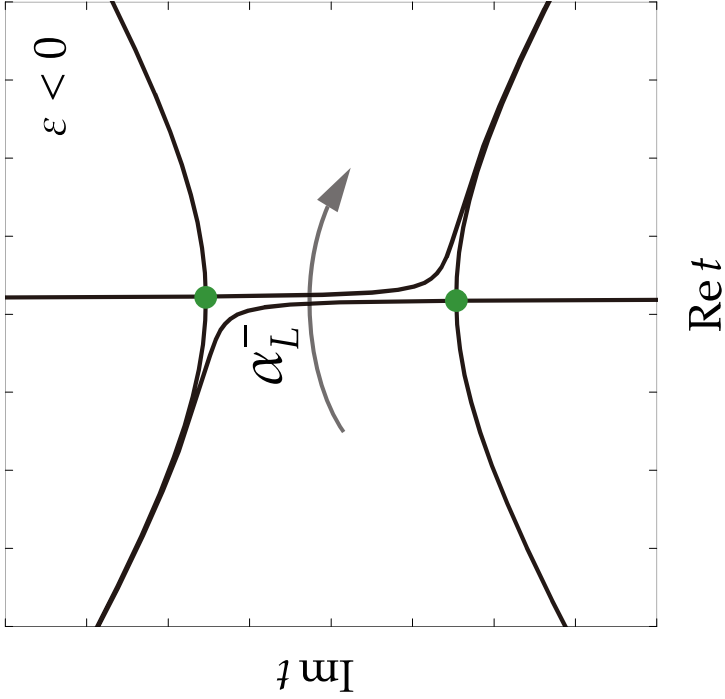


Connection across the degenerated Stokes curve

For the Stokes curve satisfying $\arg(t - t_{jk,-}) = \pi/2$ in the limit of $\varepsilon \rightarrow -0$,

$$\alpha_L^- = (2\eta)^{-\kappa_{jk,-}} \sqrt{\frac{2\pi}{\lambda_{jk,-}} \frac{\overline{c_{jk}}}{\Gamma(1 - \kappa_{jk,-})}} e^{\frac{3}{2}i\pi\kappa_{jk,-} + \frac{3}{4}i\pi} (\beta_{jk,-})^{-1},$$

$$\beta_{jk,-} = \exp\left[\frac{\eta}{i} \int_{t_{jk,-}}^{t_0} (\rho_j - \rho_k) dt\right] (t_{jk,-} - t_{jk,+})^{-2\kappa_{jk,+}} \prod_{m=1}^q (t_{jk,-} - t_{jl,m})^{-\kappa_{jl,m}} \prod_{m=1}^r (t_{jk,-} - t_{kl,m})^{\kappa_{kl,m}} \left(\frac{\lambda_{jk,-}}{2}\right)^{\kappa_{jk,-}}$$

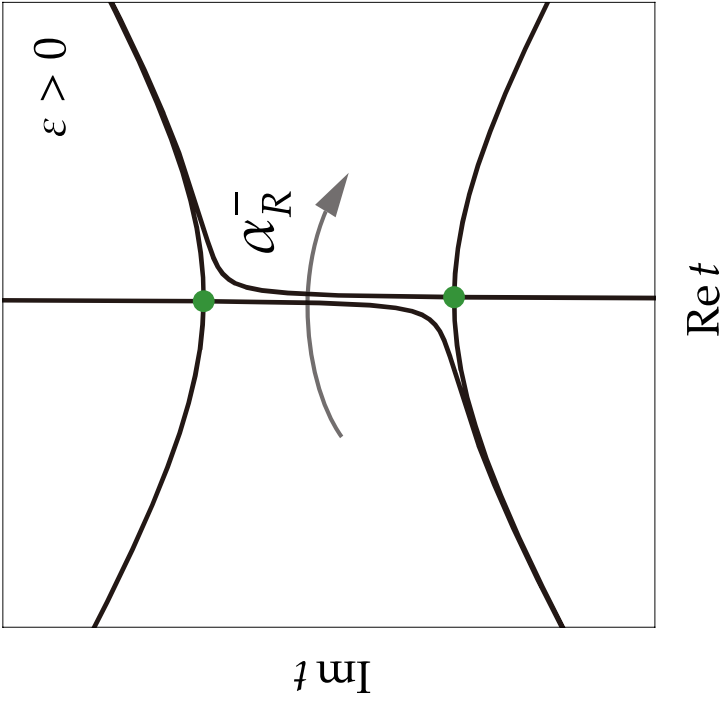
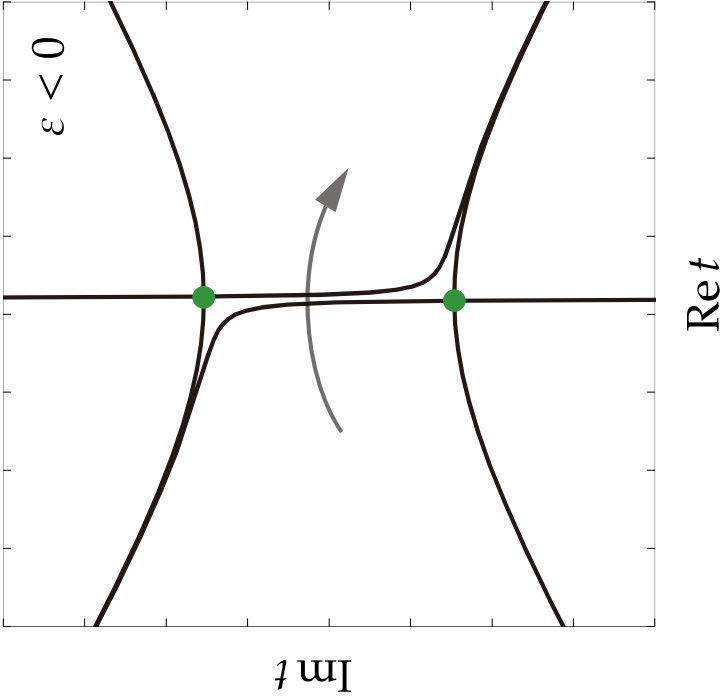


Connection across the degenerated Stokes curve

For the Stokes curve satisfying $\arg(t - t_{jk,+}) = \pi/2$ in the limit of $\varepsilon \rightarrow +0$,

$$\alpha_R^- = (2\eta)^{\kappa_{kj,+}} \sqrt{\frac{2\pi}{\lambda_{kj,+}}} \frac{c_{kj}}{\Gamma(1 + \kappa_{kj,+})} e^{-\frac{1}{2}i\pi\kappa_{kj,+} + \frac{1}{4}i\pi} (\beta_{kj,+})$$

$$\beta_{kj,+} = \exp\left[\frac{\eta}{i} \int_{t_{jk,+}}^{t_0} (\rho_k - \rho_j) dt\right] (t_{jk,+} - t_{jk,-})^{-2\kappa_{kj,-}} \prod_{m=1}^r (t_{jk,+} - t_{kl,m})^{-\kappa_{kl,m}} \prod_{m=1}^q (t_{jk,+} - t_{jl,m})^{\kappa_{jl,m}} \left(\frac{\lambda_{kj,+}}{2}\right)^{\kappa_{kj,+}}$$



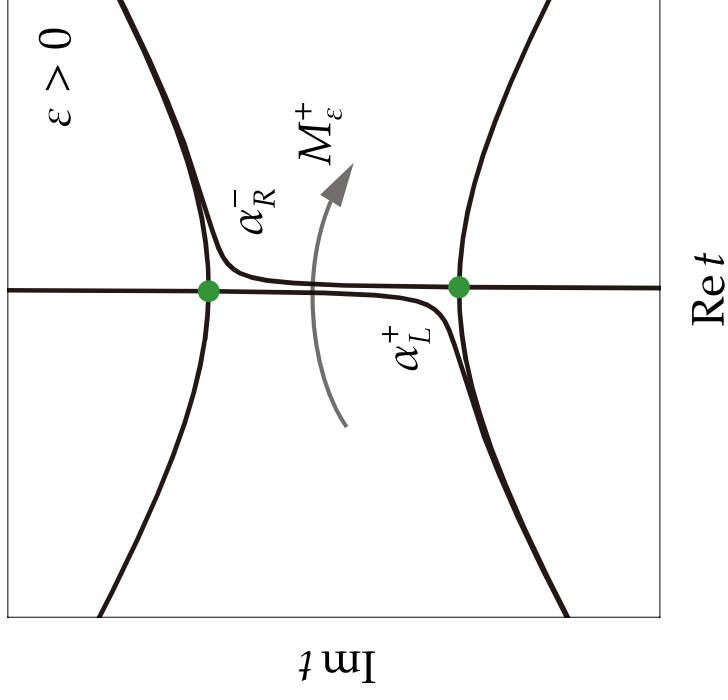
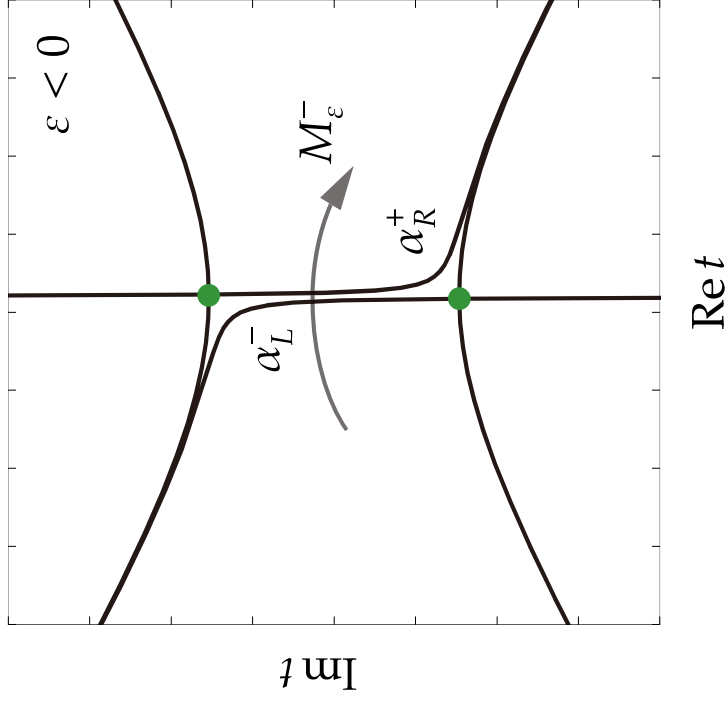
Connection across the degenerated Stokes curve

Explicit expressions for $\alpha_L^\pm, \alpha_R^\pm$ lead to

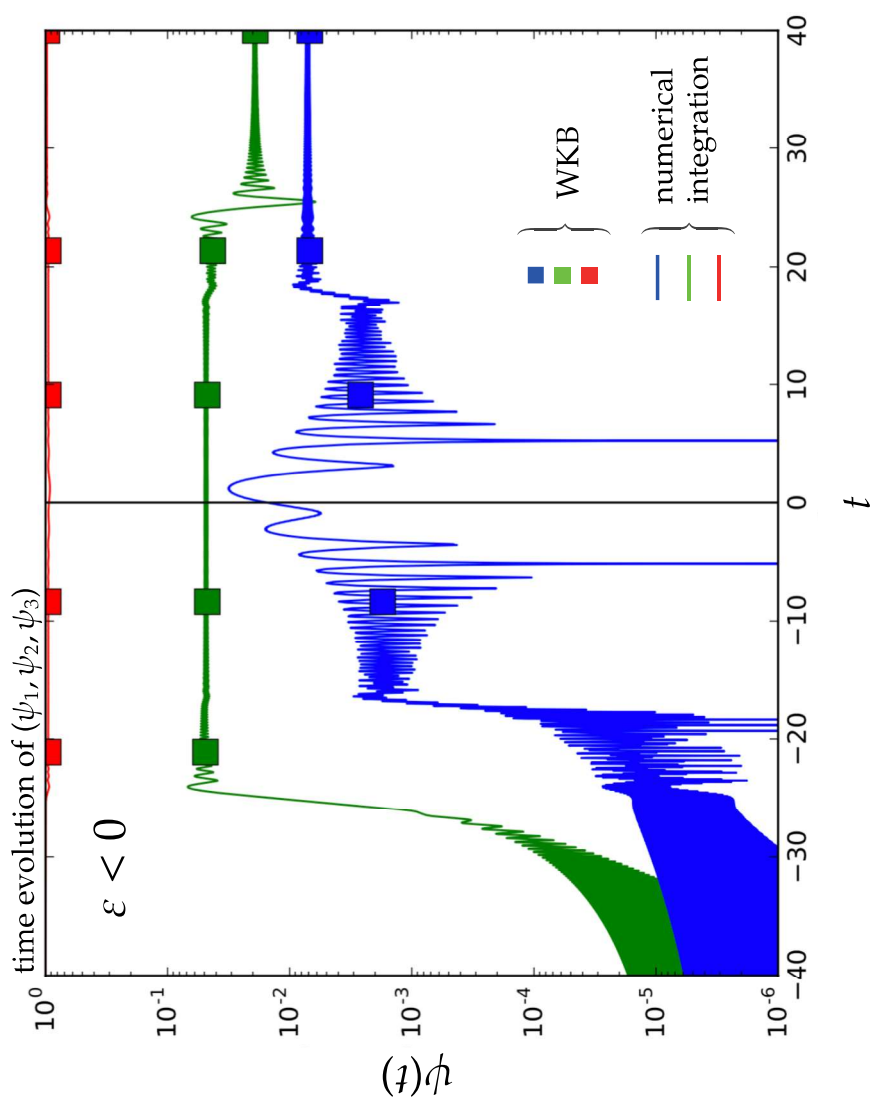
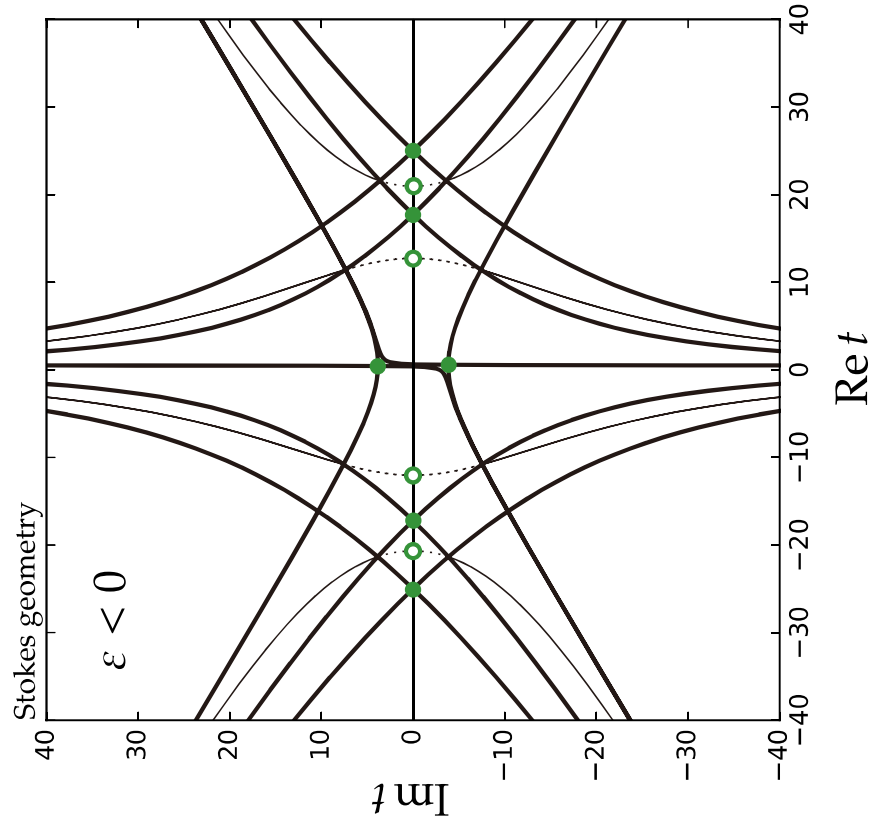
$$\lim_{\varepsilon \rightarrow -0} \alpha_L^- = \lim_{\varepsilon \rightarrow +0} \alpha_R^- =: \alpha_- \quad \lim_{\varepsilon \rightarrow -0} \alpha_R^+ = \lim_{\varepsilon \rightarrow +0} \alpha_L^+ =: \alpha_+$$

Connection matrices

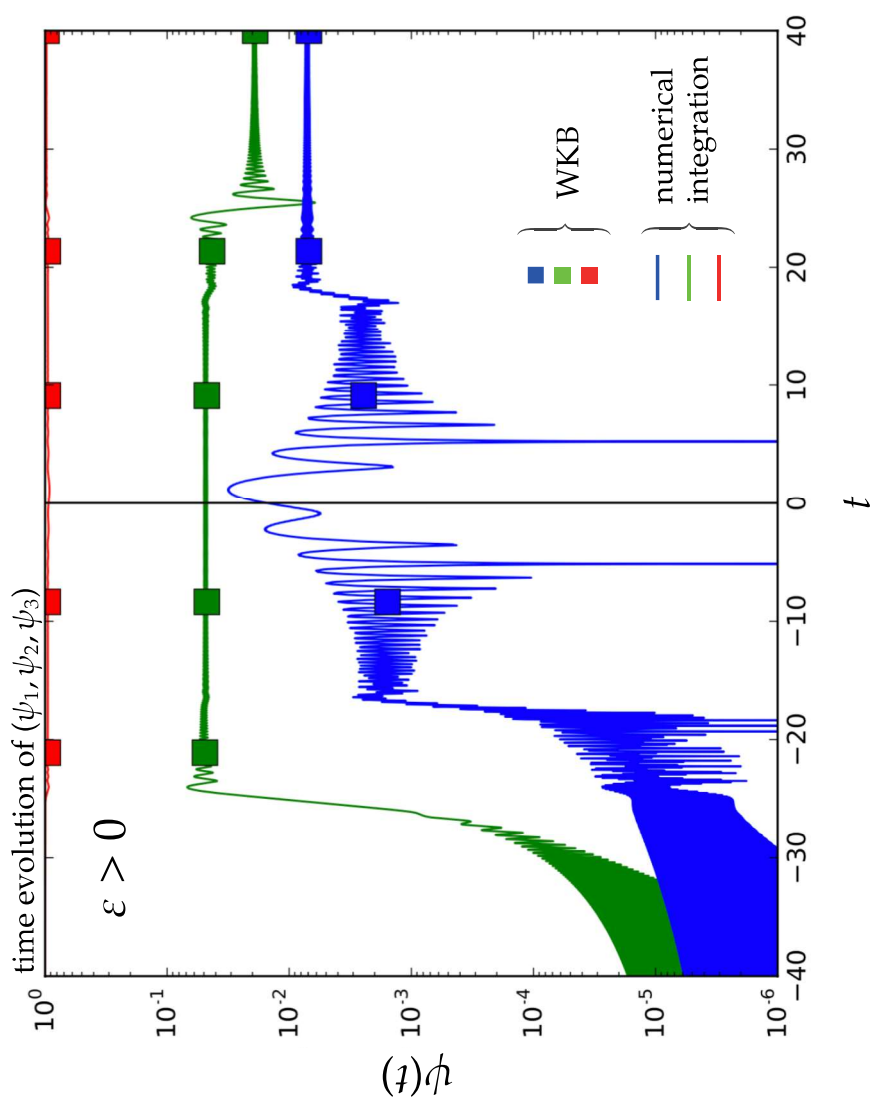
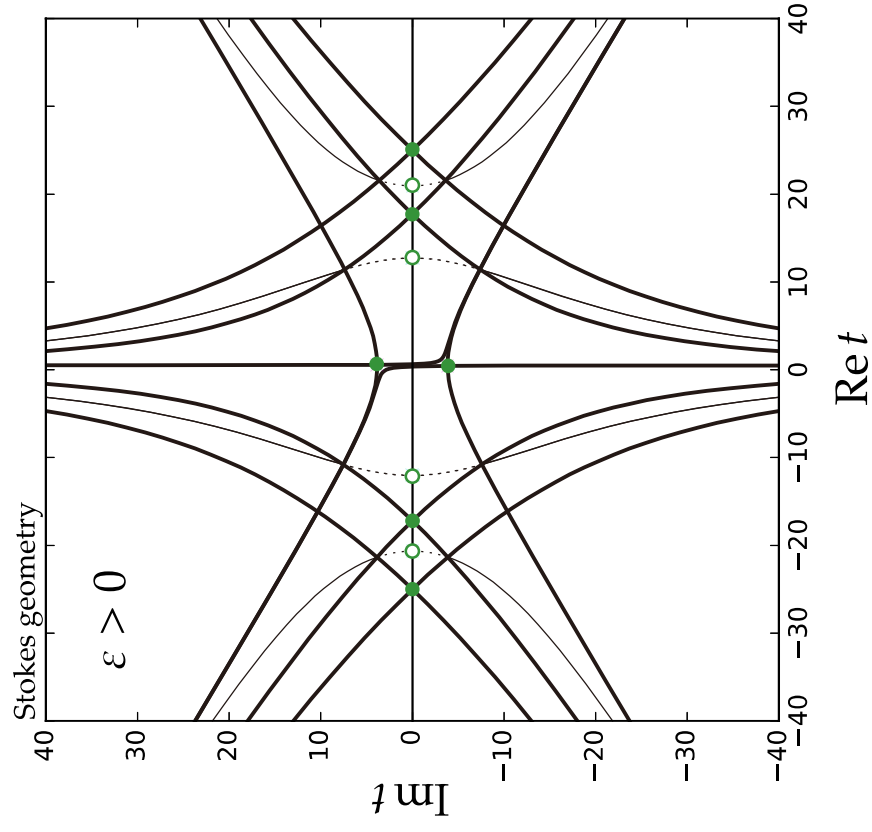
$$M^- := \lim_{\varepsilon \rightarrow -0} M_\varepsilon^- = \begin{pmatrix} 1 - \alpha_- \alpha_+ & -\alpha_- \\ \alpha_+ & 1 \end{pmatrix} \quad M^+ := \lim_{\varepsilon \rightarrow -0} M_\varepsilon^+ = \begin{pmatrix} 1 & -\alpha_- \\ \alpha_+ & 1 - \alpha_- \alpha_+ \end{pmatrix}$$



Numerical verification of the exact WKB prediction



Numerical verification of the exact WKB prediction



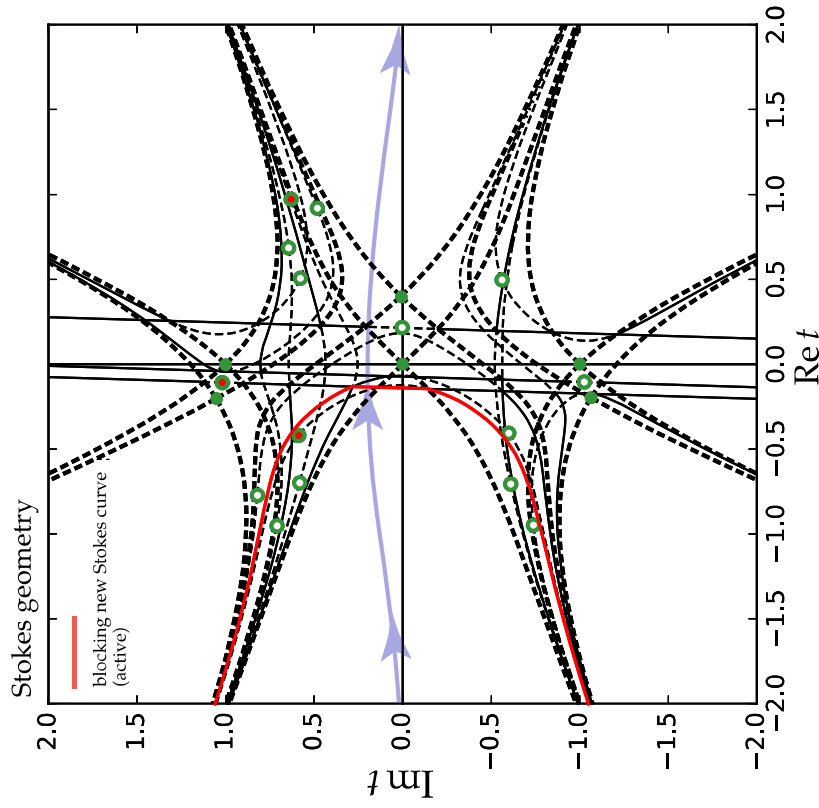
Active new Stokes curves crossing the real axis

We here examine the case where new Stokes curves cross the real axis, and

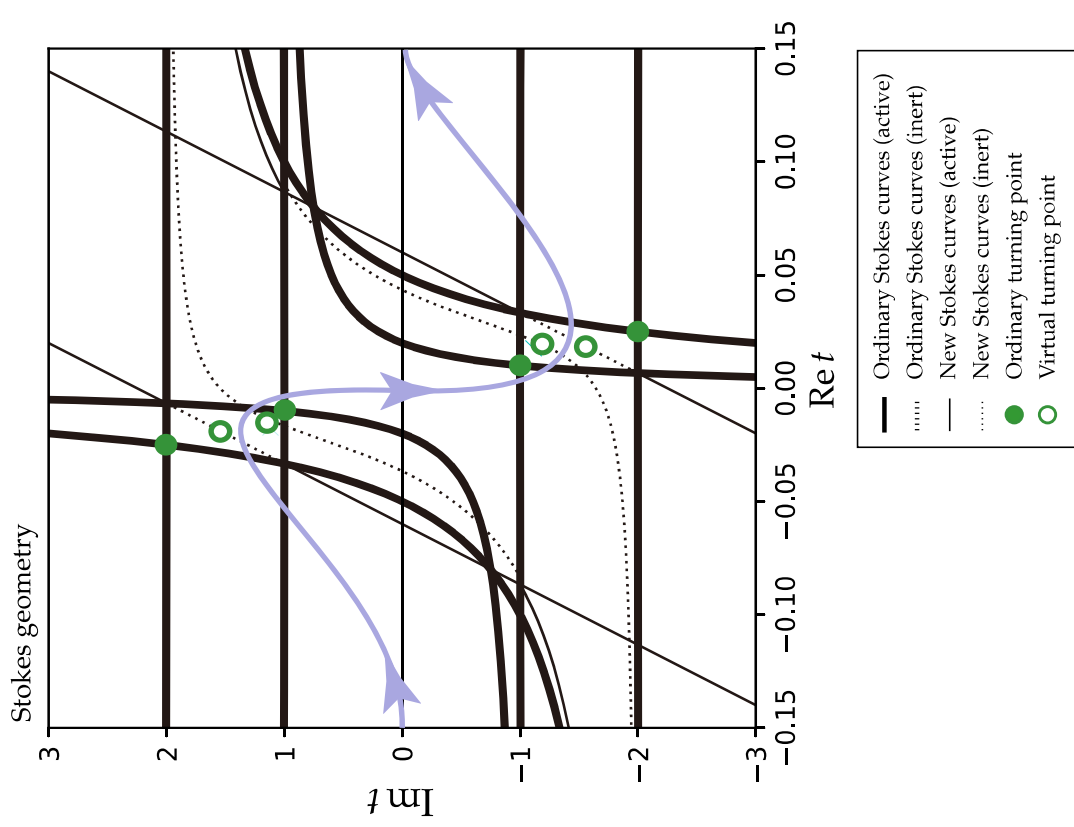
- Case 1) cannot avoid crossing new Stokes curves (Sasaki 2015)
- Case 2) a path of analytical continuation exists avoiding new Stokes curves
(AS 2006, Sasaki 2016)

Active new Stokes curves crossing the real axis

Case 1)



Case 2)



Detectability of the effect of new Stokes curves (Case 1)

Connection occurs as

$$(\psi^{(1)}, \psi^{(2)}, \psi^{(3)}) \mapsto (\psi^{(1)}, \psi^{(2)}, \psi^{(3)})M$$

where

$$M = \begin{pmatrix} 1 & \alpha_1(1 + \beta_1\beta_2) + \alpha_3\beta_1 & \alpha_3 + \alpha_1\beta_2 \\ \alpha_2 & (1 + \alpha_1\alpha_2)(1 + \beta_1\beta_2) & (1 + \alpha_1\alpha_2)\beta_2 \\ \alpha_4 & \alpha_1\alpha_4(1 + \beta_1\beta_2) + (1 + \alpha_3\alpha_4)\beta_1 & 1 + \alpha_3\alpha_4 + \alpha_1\alpha_4\beta_2 \end{pmatrix}$$

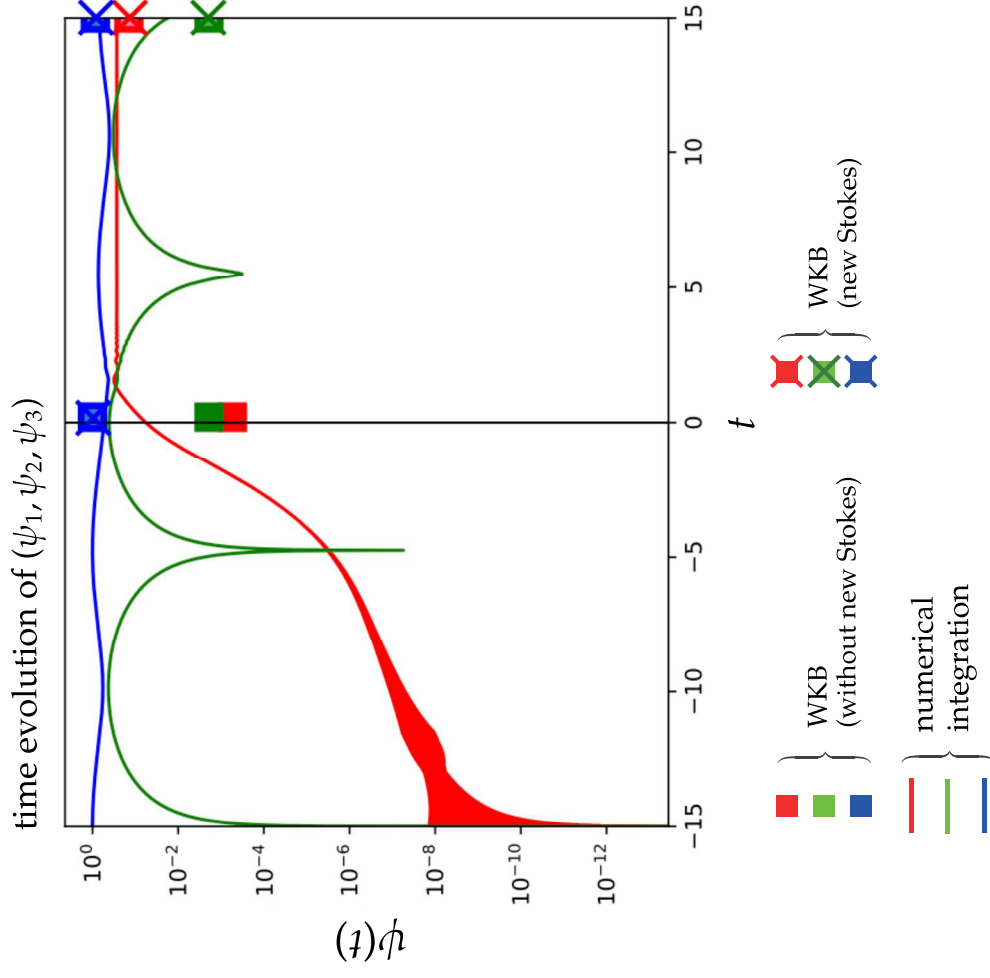
α_i : Stokes coefficient for ordinary Stokes curve

β_i : Stokes coefficient for new Stokes curve

The effect of new Stokes curves might be detected when focusing on the transition associated with (2, 3)-element, $(1 + \alpha_1\alpha_2)\beta_2 \sim \beta_2$ (Sasaki's observation)

Detectability of the effect of new Stokes curves (Case 1)

$$\eta = 1$$



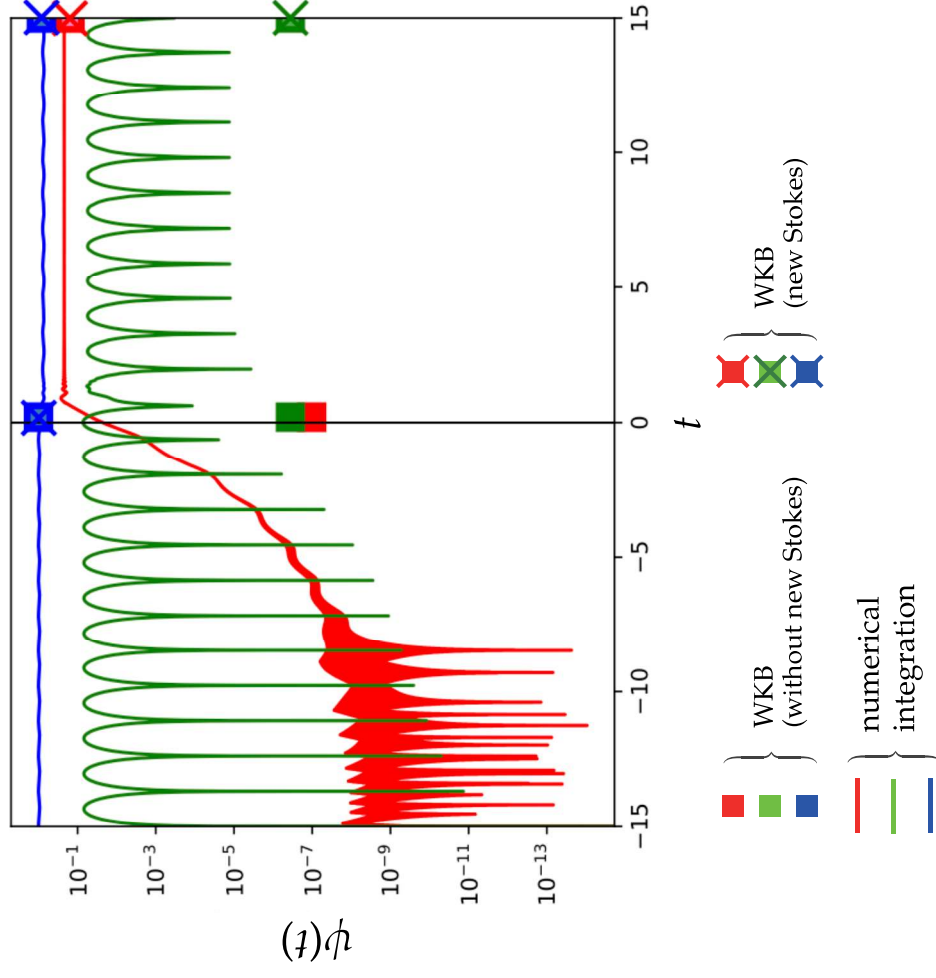
From the form of the connection matrix, the transition from **blue** to **green** is given as a result of the connection through a new Stokes curve

- No visible signature of interaction between **blue** and **green** associated with a new Stokes curve.
- Leading order WKB from **blue** to **green** does not work.

Detectability of the effect of new Stokes curves (Case 1)

$$\eta = 10$$

time evolution of (ψ_1, ψ_2, ψ_3)



From the form of the connection matrix, the transition from **blue** to **green** is given as a result of the connection through a new Stokes curve

- No visible signature of interaction between **blue** and **green** associated with a new Stokes curve.
- Leading order WKB from **blue** to **green** does not work.

Detectability of the effect of new Stokes curves (Case 2)

Connection occurs as

$$(\psi^{(1)}, \psi^{(2)}, \psi^{(3)}) \longmapsto (\psi^{(1)}, \psi^{(2)}, \psi^{(3)})M$$

where

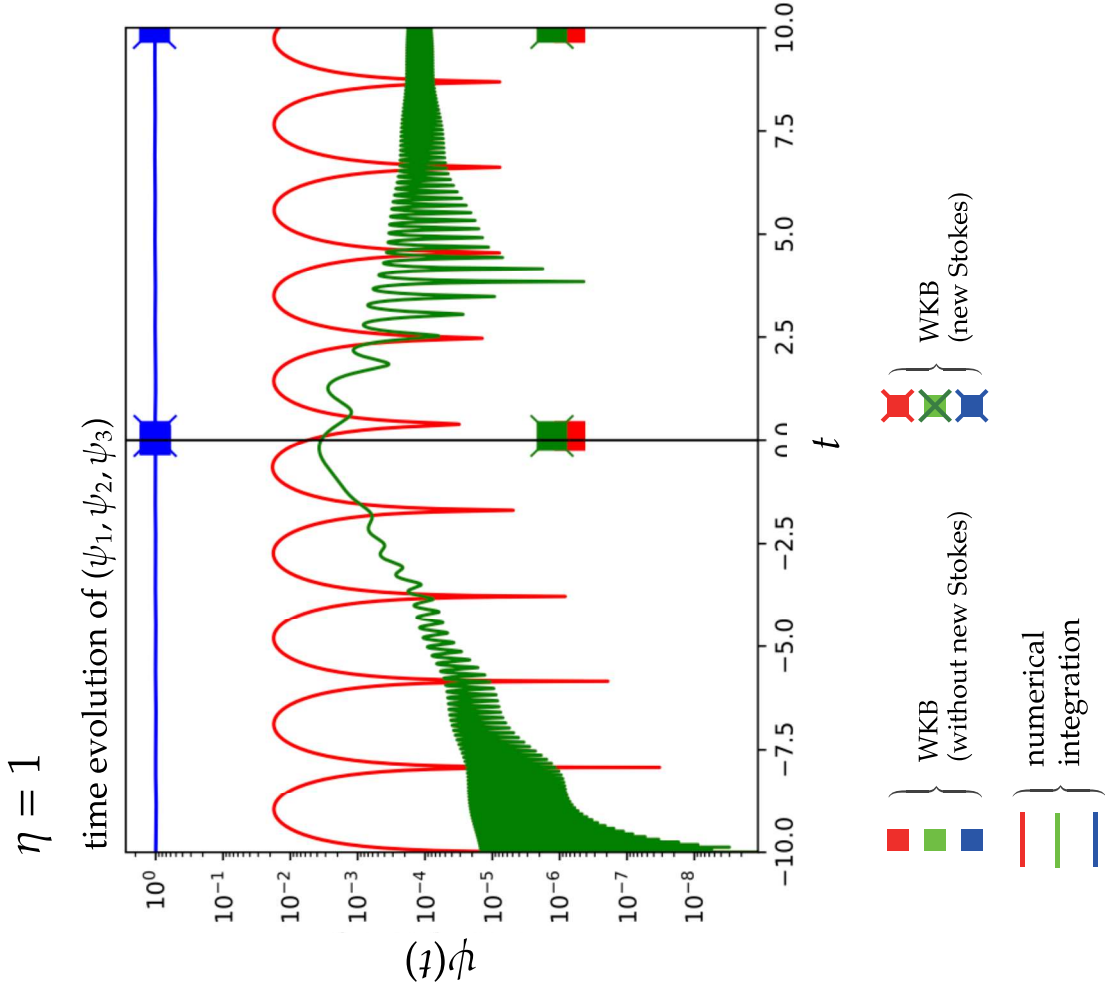
$$M = \begin{pmatrix} 1 + \beta_1\beta_2 & \alpha_2 + \alpha_1\beta_2 & \beta_2 \\ \alpha_3 + \alpha_4\beta_1 & 1 + \alpha_2\alpha_3 + \alpha_1\alpha_4 & \alpha_4 \\ \beta_1 & \alpha_1 & 1 \end{pmatrix}$$

α_i : Stokes coefficient for ordinary Stokes curve

β_i : Stokes coefficient for new Stokes curve

Since $\beta_2 \gg \alpha_4$, the effect of new Stokes curves associated with (1, 3)-element β_2 might be detected.

Detectability of the effect of new Stokes curves (Case 2)



Connection matrix:

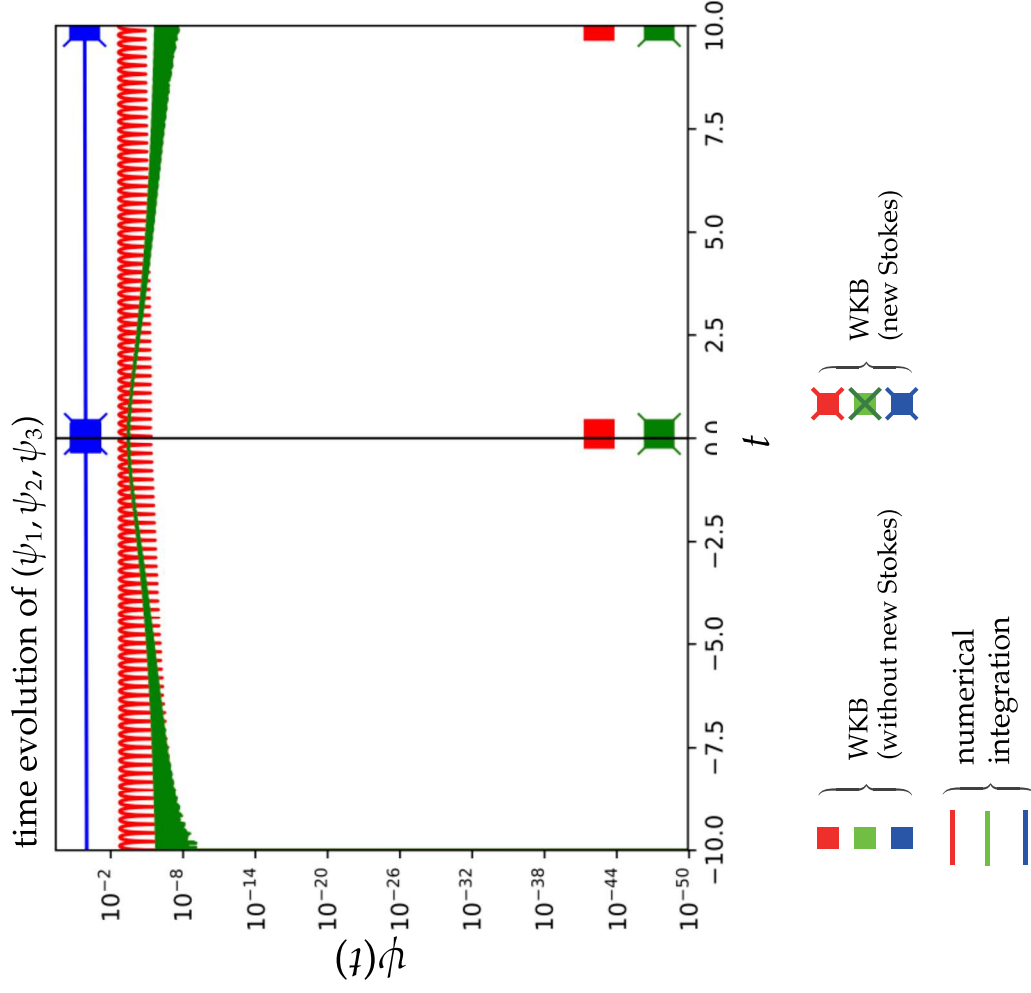
$$M = \begin{pmatrix} 1 + \beta_1\beta_2 & \alpha_2 + \alpha_1\beta_2 & \beta_2 \\ \alpha_3 + \alpha_4\beta_1 & 1 + \alpha_2\alpha_3 + \alpha_1\alpha_4 & \alpha_4 \\ \beta_1 & \alpha_1 & 1 \end{pmatrix}$$

- β_2 : (1,3) (blue→red) element
- α_4 : (2,3) (blue→green) element
- $\alpha_2 + \alpha_1\beta_2$: (1,2) (green→red) element

- No visible signature of interaction between blue and red, associated with a new Stokes curve.
- Leading order WKB from blue to red does not work.

Detectability of the effect of new Stokes curves (Case 2)

$\eta = 10$



Connection matrix:

$$M = \begin{pmatrix} 1 + \beta_1\beta_2 & \alpha_2 + \alpha_1\beta_2 & \beta_2 \\ \alpha_3 + \alpha_4\beta_1 & 1 + \alpha_2\alpha_3 + \alpha_1\alpha_4 & \alpha_4 \\ \beta_1 & \alpha_1 & 1 \end{pmatrix}$$

β_2 : (1,3) (blue→red) element

α_4 : (2,3) (blue→green) element

$\alpha_2 + \alpha_1\beta_2$: (1,2) (green→red) element

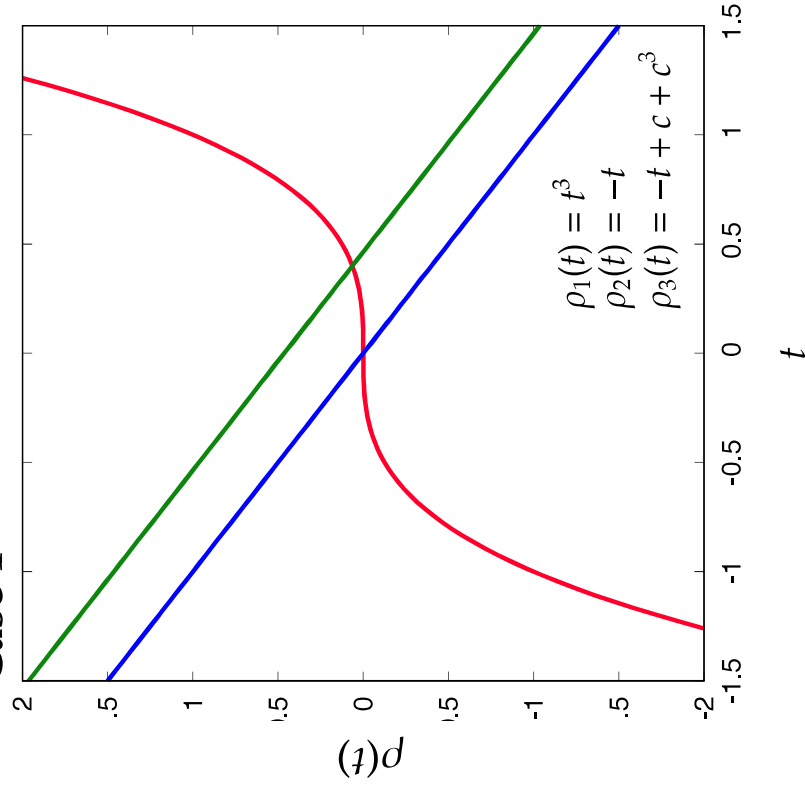
- No visible signature of interaction between blue and red, associated with a new Stokes curve.

- Leading order WKB from blue to red does not work.

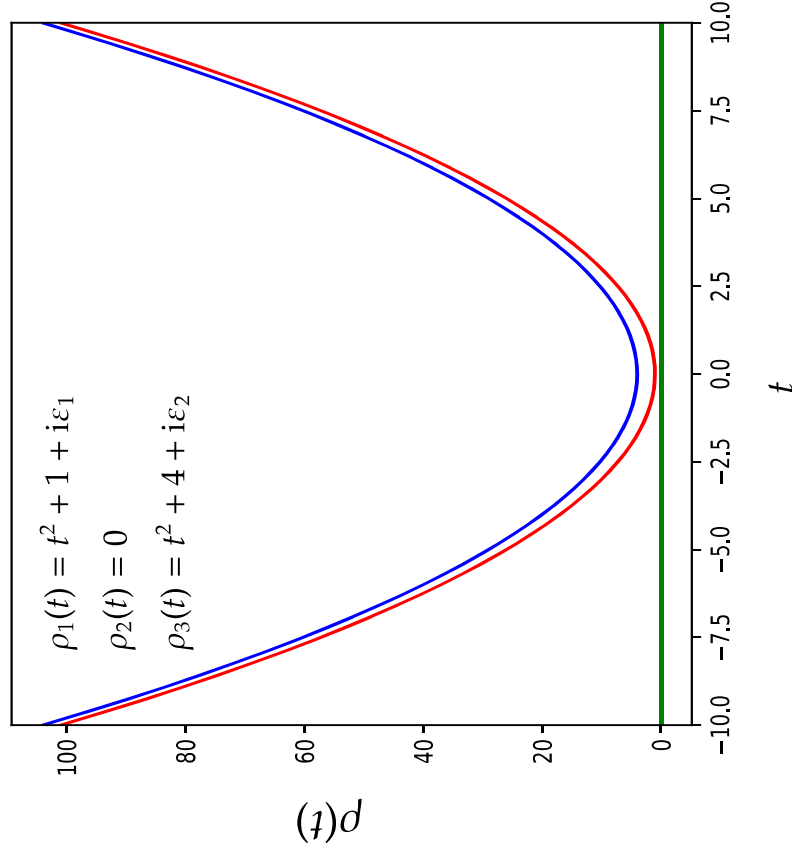
Why the leading-order WKB approximation break?

Potential curves for *blue* and *green* (Case 1), and *blue* and *red* (Case 2) are running almost in parallel, which causes the breakdown of the leading-order WKB.

Case 1

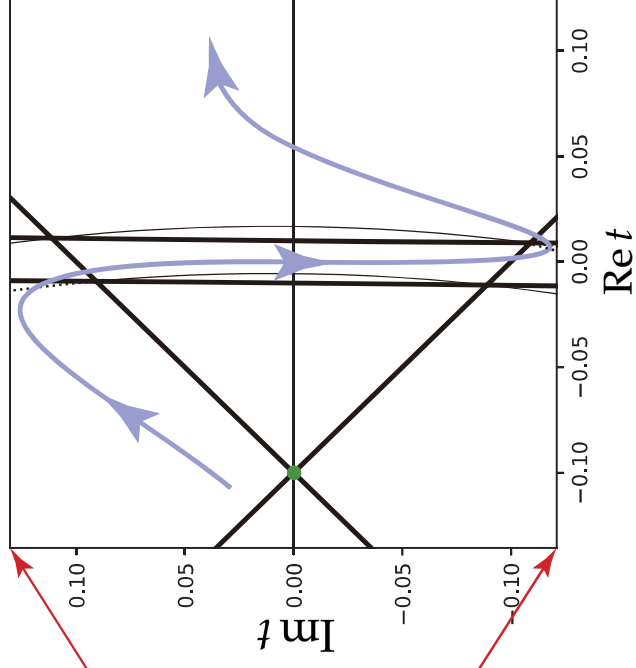
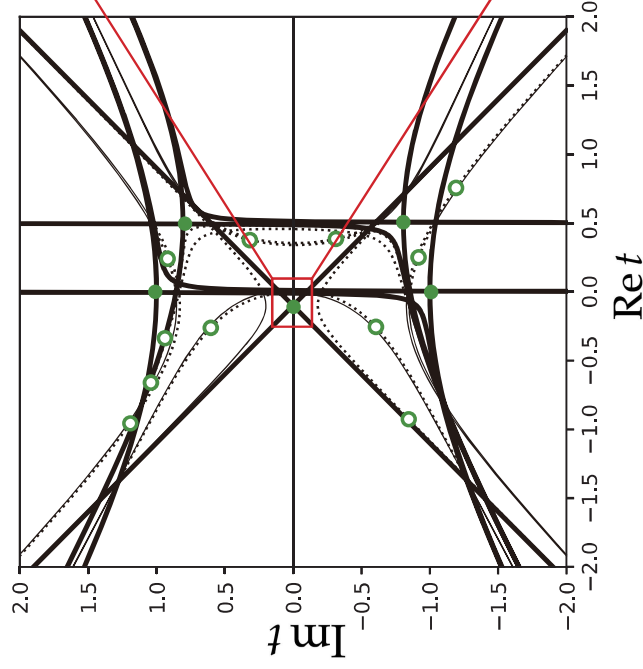
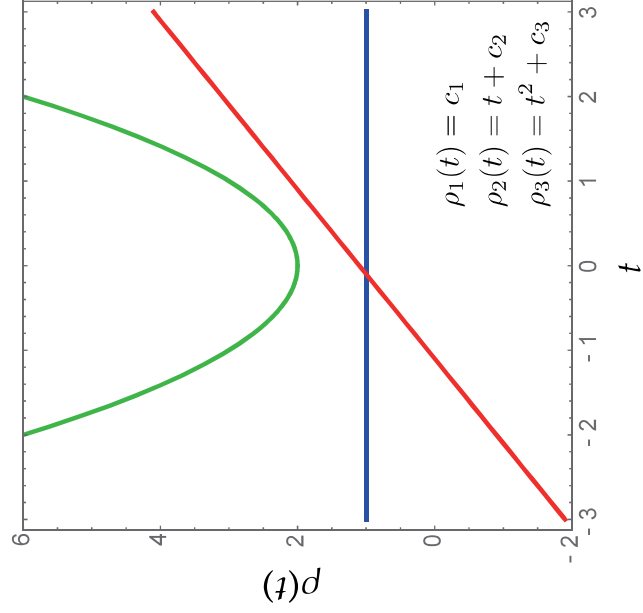


Case 2

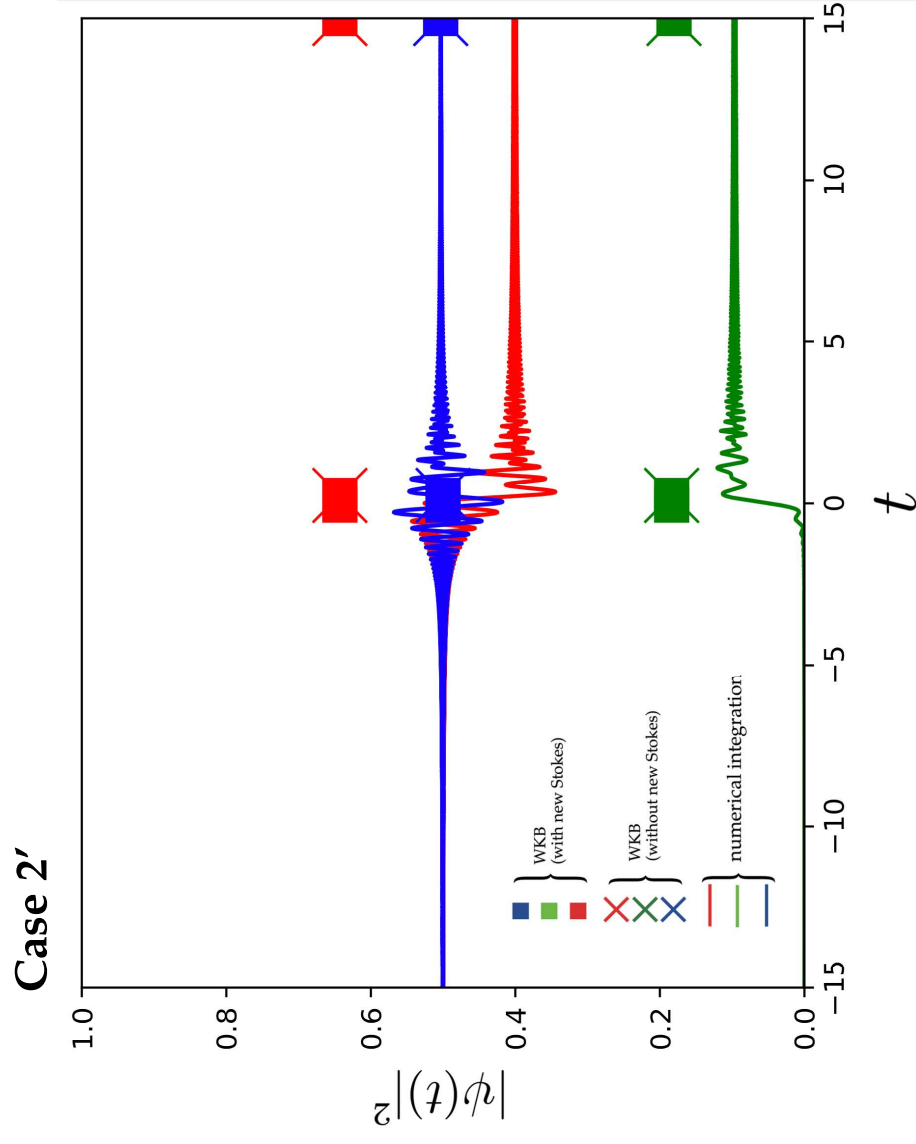


Detectability of the effect of new Stokes curves (Case 2')

Case 2'



Detectability of the effect of new Stokes curves (Case 2')



Why the leading-order WKB approximation break?

- If the virtual turning points are located far from the real axis, the amplitude of Stokes constants, which takes the form α_i (or β_i) = $\eta^{-a_i} \exp(-b_i \eta)$ in general, becomes small, thereby the contribution of new Stokes curves cannot be detected. Therefore, to have a relatively large Stokes constant, the associated virtual turning point has to be close to the real axis.
- On the other hand, our experience shows that virtual turning points and ordinary turning points move in a correlated way with the change of parameters. This means that ordinary turning points also have to be close to the real axis. However if a pair of ordinary Stokes turning points is close to each other, the leading-order WKB approximation does not work well, meaning the contribution from the new Stokes curves is hidden in the error of the leading-order WKB approximation.

Summary

We have examined the role of the new Stokes curves in the following two situations of physical origin.

1. Feynman propagator for the discrete dynamical systems

Saddle point solutions associated with the connection on active new Stokes curves are dropped due to the boundary condition, the effect of new Stokes curves does not appear explicitly.

2. Multi-state non-adiabatic transition problem

For the known examples where active new Stokes curves form a complete or partial barrier, the effect of the new Stokes curves is hidden in the error of the leading order term.